International Journal of Thermophysics, Vol. 4, No. 1, 1983

A Switch Function Applied to the Thermodynamic Properties of Steam Near and Not Near the Critical Point

H. W. Woolley[1]

Received January 4, 1983

A study is presented of the still-unsolved problem of estimating thermodynamic property values in a region intermediate between the critical region in which the scaling laws apply, and regions further from critical, where classical behavior prevails. A procedure has been developed in which a varying weighting function is used in obtaining a weighted "average" of the scaled and the classical Helmholtz free energy. Other properties are then obtained by differentiation. It is first demonstrated that it is fundamentally impossible for the "averaged" Helmholtz free energy and its first two derivatives to all be intermediate between the corresponding values from the scaled and the classical formulations. The procedure has been developed and tested for steam. The scaled function is the simple linear model of Murphy et al., the classical equation that of Pollak. The properties of power-weighted switch functions, particularly with respect to the behavior of higher-order derivatives, and the choice of the boundaries of the switching region, were examined in detail and optimized by proper choice of parameters. It is shown that a reasonably smooth transfer from the scaled to the classical region can be achieved as far as free energy, energy, and specific heat C_V are concerned. For satisfactory behavior of all second derivative properties, the two formulations need to be more compatible in the switching region than they are in the present case.

KEY WORDS: critical region; steam; thermodynamic properties; water.

1. INTRODUCTION

A somewhat strange problem arises in representing the thermodynamic properties of fluid substances. In recent years, it has become evident that the older procedures of basing estimates for the effects of interaction between molecules on equations like that of van der Waals did not actually succeed in representing properties accurately close to the critical point. The failure was evident not only in a region of coexistence of vapor and liquid

---

[1] Thermophysics Division, National Bureau of Standards, Washington, D.C. 20234, U.S.A.

0195-928X/83/0300-0051$03.00/0

just below the critical temperature but also for a limited range of temperature above for densities near the critical density. While it had once been supposed that special refinements of the old equations of state like van der Waals would be enough to take care of the problem, it has become apparent in recent years that something else is involved in the critical region. The accurate representation of properties in that region has involved something that is referred to as "scaling" or the use of a scaled equation. While this new proccedure does very well in a limited region near the critical point, and while there may be ways of extending the representation with considerable accuracy somewhat further way, it still appears that some unsolved problems remain in regard to extending the critical region treatment to the entire region of interest. This would involve densities of the fluid that would range all the way from zero up into high density regions such as are typical of the liquid.

It is to be noted that equations of state of such classical forms as are typified by that of van der Waals, and those that are equivalent to sums of virial series, are generally successful over broad ranges of density and temperature that would cover all regions of interest for engineering uses, other than the critical region. It becomes of interest to see if there is a way of making use of these two representations, the scaled and the classical, which are successful in their respective regions, and to do something which would in some way bridge over the intermediate region, so that we might have a numerically acceptable practical way of representing properties throughout the entire region of interest. An attempt is to be presented at producing a smooth continuation of such a type between two regions, one near the critical point and the other far away.

2. IDEA OF A SWITCHING FUNCTION

Chapela and Rowlinson [1] applied a switching procedure directly to pressure data for carbon dioxide and methane according to the equation

$$p = f(r)P_A + \left[1 - f(r)\right]P_S \tag{1}$$

with $f(r)$ as a specially chosen function having the value "zero" at the critical point and rising substantially to the value "one" far away from the critical point. The quantity r is one of the parametric variables, r and θ, as used in simple scaled representations [2, 3]. Values for related thermodynamic properties at higher density, such as for the liquid, were apparently arrived at by numerical, or tabular, integration processes. Complete results of integration as an overall formulation in global closed form do not appear to have been given by Chapela and Rowlinson [1].

In the present approach the procedure is one of taking the Helmholtz free energy representations for the two separate types of formulation and forming a linear combination of the two quantities, using a variable weighting function. A suggestion for such a procedure was made in 1969 by Kestin [4]. The advantage is that all other thermodynamic properties follow by differentiation.

The arrangement of the weighting function in the present case is made in such a way that it has its full value, that is, the number "1" for a considerable region around the critical point, and it has the other extreme value, "0," for the total region far away from the critical point. Then there is an intermediate band or range of variables in which the weighting function varies between its full value of 1 and its smallest value of 0.

This may be shown explicitly for the Helmholtz free energy A, if A_I is satisfactory in region I and A_{II} is satisfactory in region II, by

$$A = g_1 A_I + g_2 A_{II} = g A_I + (1 - g) A_{II} \tag{2}$$

where $g = g_1$ and $g_2 = 1 - g_1$. In regions other than I and II combined it is hoped that g may be so chosen as to provide favorable agreement with observation. The variable weighting function g may well be termed a switching function if it has the value unity over some large region of temperature and density and the value zero in some other large region. The more broadly applicable term "blend function" may perhaps be preferable under some circumstances, particularly if g were to be so defined as to not quite reach the stated endpoint values.

All of the quantities of interest for thermodynamic properties are obtained from the free energy by suitable differentiations, with other numerical processes that may be indicated algebraically. The differentiations are partly with respect to temperature and partly with respect to density. Since the weighting function is included in the representation of the total free energy, there will necessarily be derivatives of that weighting function coming into the expressions for the various derived quantities. The derivatives of g are to be indicated here according to the abbreviations

$$\begin{aligned} g_T &= T(\partial g/\partial T)_\rho, \qquad & g_{TT} &= T^2(\partial^2 g/\partial T^2)_\rho \\ g_\rho &= \rho(\partial g/\partial \rho)_T, \qquad & g_{\rho\rho} &= \rho^2(\partial^2 g/\partial \rho^2)_T \end{aligned} \tag{3}$$

and

$$g_{T\rho} = T\rho\,\partial^2 g/\partial T\partial\rho$$

with ρ to indicate density and T to indicate absolute temperature.

Various derived thermodynamic quantities follow quite naturally. In writing expressions for them, various well-known identities have been used, such as

$$
\begin{aligned}
T\partial(-A/RT)/\partial T &= E/RT \\
\partial\big(T^2\partial(-A/RT)/\partial T\big)/\partial T &= C_v/R \qquad (4) \\
-\rho\partial(-A/RT)/\partial\rho &= PV/RT = Z
\end{aligned}
$$

Among the directly derived quantities is the internal energy, E, indicated by

$$
E/RT = g(E/RT)_I + (1-g)(E/RT)_{II} + g_T\big[(-A_I(RT) - (-A_{II}/RT)\big] \qquad (5)
$$

We also have the so-called molar compressibility factor $Z = PV/RT$, given by

$$
Z = gZ_I + (1-g)Z_{II} - g_\rho\big[(-A_I(RT) - (-A_{II}/RT)\big] \qquad (6)
$$

and the molar heat capacity at constant volume

$$
\begin{aligned}
C_v/R = g(C_v/R)_I + (1-g)(C_v/R)_{II} + 2g_T\big[(E/RT)_I - (E/RT)_{II}\big] \\
+ (2g_T + g_{TT})\big[(-A_I/RT) - (-A_{II}/RT)\big] \qquad (7)
\end{aligned}
$$

Other quantities are also of possible usefulness. There are

$$
\begin{aligned}
\rho(\partial Z/\partial\rho)_T = g\rho(\partial Z_I/\partial\rho)_T + (1-g)\rho(\partial Z_{II}/\partial\rho)_T + 2g_\rho\big[Z_I - Z_{II}\big] \\
- (g_\rho + g_{\rho\rho})\big[(-A_I/RT) - (-A_{II}/RT)\big] \qquad (8)
\end{aligned}
$$

and

$$
\begin{aligned}
T(\partial Z/\partial T)_\rho = gT(\partial Z_I/\partial T)\rho + (1-g)T(\partial Z_{II}/\partial T)_\rho \\
+ g_T\big[Z_I - Z_{II}\big] - g_{T\rho}\big[(-A_I/RT) - (-A_{II}/RT)\big] \\
- g_\rho\big[(E_I/RT) - (E_{II}/RT)\big] \qquad (9)
\end{aligned}
$$

The quantities given by the last two of the preceding equations are useful in obtaining the heat capacity at constant pressure,

$$C_p/R = C_v/R + \left[Z + T(\partial Z/\partial T)\right]^2/\left[Z + \rho(\partial Z/\partial \rho)\right] \qquad (10)$$

Other quantities of interest can be generated in corresponding ways. From the expression for the compressibility factor, the pressure is seen to be given by

$$P = gP_I + (1 - g)P_{II} - g_\rho\left[(-A_I/RT) - (-A_{II}(RT)\right]RT/V \qquad (11)$$

For a suitable approach to the switching process as here envisioned, there is a need to indicate the region within which the switching is to occur. In the present attempt, a simple variable s is to be used to indicate "distance" from the critical point. The value of s is to be zero at the critical point and to increase to larger values for all directions in moving away from the critical point. Two special fixed values, s_1 and s_2, are chosen. If s is less than the lesser, s_1, then the region I is implied, where $g = 1$; if s is larger than s_2, then region II is implied, where $g = 0$. For s between s_1 and s_2, the region of a varying weighting or switching function is involved.

This variability leads to special contributions to thermodynamic functions as indicated via Eqs. (3)–(11). The involvement of derivatives related to the distance function s occurs according to the following relations:

$$\begin{aligned}
g_T &= T(\partial g/\partial T)_\rho = (dg/ds)(T\partial s/\partial T) \\
g_{TT} &= T^2(\partial^2 g/\partial T^2)_\rho = (d^2g/ds^2)(T\partial s/\partial T)^2 + (dg/ds)(T^2\partial^2 s/\partial T^2) \\
g_\rho &= \rho(\partial g/\partial \rho)_T = (dg/ds)(\rho\partial s/\partial \rho) \qquad (12) \\
g_{\rho\rho} &= \rho^2(\partial^2 g/\partial \rho^2)_T = (d^2g/ds^2)(\rho\partial s/\partial \rho)^2 + (dg/ds)(\rho^2\partial^2 s/\partial \rho^2) \\
g_{T\rho} &= T\rho\partial^2 g/\partial T\partial \rho = (d^2g/ds^2)(T\partial s/\partial T)(\rho\partial s/\partial \rho) \\
&\quad + (dg/ds)(T\rho\partial^2 s/\partial T\partial \rho)
\end{aligned}$$

These equations will bring in considerable complexity to the situation, such as the local dependence of the so-called distance s on temperature and density, a topic to be explored below.

3. GENERAL CONSIDERATIONS

Intuitively, one might set as a goal for proper "blending" that the blended free energy and its first and second derivatives be intermediate between thoese of the two free energy surfaces being blended. This goal, however, cannot be attained, as will now be shown. ,As an example, one may consider the behavior of the blended free energy, the energy, and the specific heat at constant volume for temperatures above critical. In the process of calculating heat capacity at constant volume for temperatures above the critical, difficulties may arise due to the behavior of the scaled and analytic representations of the free energy and the internal energy. According to Eq. (7), the differences in these "energies" are multiplied by derivatives of the switching function g in obtaining the total heat capacity. Thus, the blended specific heat may get out of the bounds in regions where derivatives of g are large, especially when the analytic and scaled free energy surfaces are not sufficiently close. In fact, the relationship of the two individual free energy surfaces is of crucial importance in obtaining satisfactorily blended derived properties, as will be demonstrated graphically. In Fig. 1 the difference $\Delta(-A/RT)_{sc\text{-}cl} = (-A/RT)_{(\mathrm{scaled})} - (-A/RT)_{(\mathrm{classical})}$ is shown schematically, plotted versus $x = 1/T$. In such an Arrhenius type graph [5], the slope is a difference in internal energy, appearing as $\Delta E/R$, and the derivative of this slope versus temperature is the difference in heat capacities, $\Delta C_v/R$. The blend curve is assumed to

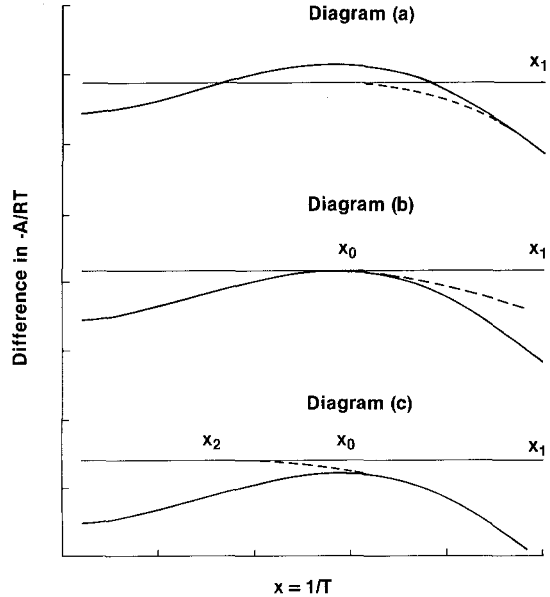

Fig. 1. Illustrative diagrams of differences in $-A/RT$ between scaled and classical formulations under conditions involving simple curves close to tangency, plotted vs $1/T$.

remain inside the region between upper and lower bounds of the $\Delta(-A/RT)_{sc\text{-}cl}$ curve and the zero axis within the intended switching region. The three diagrams of Fig. 1 show three possible cases of simple curves close to tangency, with one curve as a zero axis cutting across the other curve in diagram (a), tangent to the curve in diagram (b), and not quite contacting the curve in diagram (c). At small x, or high temperature, the acceptable formulation is the classical, represented by the zero axis.

In diagram (a), a case is considered in which the slope of a supposed blend curve, shown as a dashed line, is made less in absolute magnitude than that of the original $\Delta(-A/RT)_{sc\text{-}cl}$ curve so that the blended energy is intermediate between E_{sc} and E_{cl}. With tangency taken to occur at $x = x_1$, the dashed curve is everywhere more nearly flat than the original curve, except at its terminus, where the slopes are identical. However, to achieve tangency, the second derivative for the dashed curve near $x = x_1$ is excessive, and the blend specific heat is not intermediate between scaled and classical values in this locality. From the relative positions of the original and the dashed curve, it may be inferred that a zero axis intersecting in the switching region is not compatible with acceptable $(C_v/R)_{\text{blend}}$ values. It may be noted that this also formally covers the still less favorable case of an abrupt crossing in which a capability for approximate tangency in the vicinity is not involved.

In diagram (b), a hypothetical case is considered in which the $\Delta(-A/RT)_{sc\text{-}cl}$ curve is tangent to the zero axis at some value of x, called x_0. With blending considerations in mind, a dashed curve is also shown, tangent at x_0, but with its second derivative everywhere intermediate between values for the first curve and the zero axis. It is clear that the dashed curve also will have a slope intermediate between the slopes of the first or $\Delta(-A/RT)_{sc\text{-}cl}$ curve and the zero axis. With curves of simple structure, however, the dashed curve cannot become tangent to the first curve at any x greater than x_0, such as indicated by x_1 in the diagram. Any modification of the dashed curve to give a local approach to tangency at a point x would require a local curvature not compatible with the assumption of intermediacy of C_v/R between values for scaled and classical curves. Thus, the initial assumption of tangency of the $\Delta(-A/RT)_{sc\text{-}cl}$ curve with the zero axis does not appear compatible with acceptable $(C_v/R)_{\text{blend}}$ values throughout a finite switching interval.

In the case of diagram (a), a straightforward attempt to apply an actual switch function g would give a blend curve passing through the intersection of the primary curve and the zero axis but "curling around" appreciably to achieve tangency with the zero axis toward the left and with the primary curve toward the right of x_1. In the case of diagram (b), the use of a switching region with x_0 and x_1 as boundaries would lead to a blend curve roughly as shown but requiring undesirable local curvatures to achieve tangency at both x_0 and x_1. In neither (a) nor (b) would the curvature remain throughout between that of the primary curve and the zero axis. This indicates that $(C_v/R)_{\text{blend}}$ would not remain intermediate between the two formulations throughout the switching region.

In diagram (c), a case is considered in which $\Delta(-A/RT)_{sc\text{-}cl}$ has its least but finite departure from the zero axis at some value of $1/T$, shown as x_0. For the blend value for C_v/R to be intermediate between the scaled and classical values, the second derivative for the dashed or blend $\Delta(-A/RT)$ curve must be in the range from zero to the second derivative value for the $\Delta(-A/RT)_{sc\text{-}cl}$ curve. A dashed curve is shown for a plausible choice for such a curve, with the desired property of intermediate second derivatives or intermediate C_v/R values. From an examination of the diagram it is evident, however, that the slope of the intermediate curve is not intermediate between the slopes of the $\Delta(-A/RT)_{sc\text{-}cl}$ curve and the zero axis; therefore, the blend energy will not be intermediate between the two energies. This may be acceptable, if C_v/R and not E/R values are the experimental data fitted. Thus, it is not possible for the free energy to vary smoothly from one surface to the other while both internal energy and specific heat remain within the bounds set by the two surfaces.

4. CHOICE OF A SWITCHING FUNCTION

The following form was studied for the switching function:

$$g = x^m/\left[x^m + (1 - x)^m\right] \tag{13}$$

where $x = (s_2 - s)/(s_2 - s_1)$, and the range $s_1 < s < s_2$ is assumed. This gives g decreasing from unity at $s = s_1$ to zero at $s = s_2$. The exponent m may be chosen as any convenient integer. Tables I, II, and III give values of g and its first and second derivatives for several values of m from $m = 3$ to $m = 8$, also shown in Figs. 2, 3, and 4. In accord with Eqs. (3)–(12), the derivatives of g may make large contributions to the properties obtained by differentiation processes. The values for d^2g/ds^2 for $m = 3$ near $s = s_1$ and $s = s_2$, the end points of the table, are seen to start away from zero somewhat abruptly. The behavior for larger values of m may be more acceptable, since the corresponding changes occur less abruptly.

A difficulty in using larger values for m is apparent in examining values for d^2g/ds^2 in Table III. The second derivative changes from a large negative to a large positive value in a small range of x around the midpoint of the interval. Although larger values of m are the ones most favorable for

Table I. Values for a Switch Function g for Several Values of m, Where $g = W_1/(W_1 + W_2)$ and $W_i = h_i^m$, with $h_1 = s_2 - s$, $h_2 = s - s_1$ and $s_2 - s_1 = 1$

$s - s_1$	$m = 3$	$m = 4$	$m = 5$	$m = 6$	$m = 7$	$m = 8$
0	1.	1.	1.	1.	1.	1.
0.5	0.999854	0.999992	0.9999996	0.99999998	0.999999999	1.
0.1	0.998630	0.999848	0.999983	0.999998	0.9999998	0.99999998
0.15	0.994534	0.999031	0.999829	0.999970	0.999995	0.999999
0.2	0.984615	0.996109	0.999024	0.999756	0.999939	0.999985
0.25	0.964286	0.987805	0.995902	0.998630	0.999543	0.999848
0.3	0.927027	0.967365	0.985748	0.993842	0.997351	0.998863
0.35	0.864961	0.922453	0.956694	0.976206	0.987046	0.992983
0.4	0.771429	0.835052	0.883636	0.919284	0.944708	0.962447
0.45	0.646117	0.690548	0.731717	0.769240	0.802928	0.832767
0.5	0.5	0.5	0.5	0.5	0.5	0.5
0.55	0.353883	0.309452	0.268283	0.230760	0.197072	0.167233
0.6	0.228571	0.164948	0.116364	0.080706	0.055292	0.037553
0.65	0.135039	0.077547	0.043306	0.023794	0.012954	0.007017
0.7	0.072973	0.032635	0.014252	0.006158	0.002649	0.001137
0.75	0.035714	0.012195	0.004098	0.001370	0.000457	0.000152
0.8	0.015385	0.003891	0.000976	0.000244	0.000061	0.000015
0.85	0.005466	0.000969	0.000171	0.000030	0.000005	0.0000009
0.9	0.001370	0.000152	0.000017	0.000002	0.0000002	0.00000002
0.95	0.000146	0.000008	0.0000004	0.00000002	0.000000001	0.0000000001
1.	0	0	0	0	0	0

Table II. Values of the First Derivative, dg/ds, Where g is the Switch Function of Table I

$s - s_1$	$m = 3$	$m = 4$	$m = 5$	$m = 6$	$m = 7$	$m = 8$
0	0	0	0	0	0	0
0.05	− 0.009205	− 0.000646	− 0.000043	− 0.0000027	− 0.0000002	− 0.0000001
0.1	− 0.045600	− 0.006772	− 0.000941	− 0.000125	− 0.000016	− 0.000002
0.15	− 0.127899	− 0.030367	− 0.006709	− 0.001421	− 0.000293	− 0.000059
0.2	− 0.284024	− 0.096900	− 0.030458	− 0.009151	− 0.002670	− 0.000763
0.25	− 0.551020	− 0.256990	− 0.108842	− 0.043776	− 0.017055	− 0.006501
0.3	− 0.966399	− 0.601332	− 0.334502	− 0.174866	− 0.088052	− 0.043258
0.35	− 1.540269	− 1.257726	− 0.910559	− 0.612605	− 0.393436	− 0.245036
0.4	− 2.204082	− 2.295674	− 2.142149	− 1.854817	− 1.523504	− 1.204764
0.45	− 2.771515	− 3.453599	− 3.965799	− 4.303270	− 4.475326	− 4.501532
0.5	− 3.	− 4.	− 5.	− 6.	− 7.	− 8.
0.55	− 2.771515	− 3.453599	− 3.965799	− 4.303270	− 4.475326	− 4.501532
0.6	− 2.204082	− 2.295674	− 2.142149	− 1.854817	− 1.523504	− 1.204764
0.65	− 1.540269	− 1.257726	− 0.910559	− 0.612605	− 0.393436	− 0.245036
0.7	− 0.966399	− 0.601332	− 0.334502	− 0.174866	− 0.088052	− 0.043258
0.75	− 0.551020	− 0.256990	− 0.108842	− 0.043776	− 0.017055	− 0.006501
0.8	− 0.284024	− 0.096898	− 0.030458	− 0.009151	− 0.002670	− 0.000763
0.85	− 0.127899	− 0.030367	− 0.006709	− 0.001421	− 0.000293	− 0.000059
0.9	− 0.045600	− 0.006772	− 0.000941	− 0.000125	− 0.000016	− 0.000002
0.95	− 0.009205	− 0.000646	− 0.000043	− 0.0000027	− 0.0000002	− 0.00000001
1.	0	0	0	0	0	0

Table III. Values of the Second Derivative, d^2g/ds^2, Where g is the Switch Function of Table I

$s - s_1$	$m = 3$	$m = 4$	$m = 5$	$m = 6$	$m = 7$	$m = 8$
0	0	0	0	0	0	0
0.05	− 0.406804	− 0.042170	− 0.003669	− 0.000288	− 0.0000212	− 0.00000148
0.1	− 1.110491	− 0.240689	− 0.043903	− 0.007248	− 0.001120	− 0.0001652
0.15	− 2.274304	− 0.784115	− 0.226182	− 0.059072	− 0.014458	− 0.003379
0.2	− 4.096495	− 2.040226	− 0.835739	− 0.308672	− 0.106784	− 0.035284
0.25	− 6.717201	− 4.663426	− 2.588410	− 1.280245	− 0.590657	− 0.259959
0.3	− 9.950052	− 9.560950	− 7.100163	− 4.601562	− 2.751791	− 1.561788
0.35	− 12.794482	− 17.025615	− 17.078258	− 14.579929	− 11.273252	− 8.172582
0.4	− 13.119534	− 23.725913	− 32.456799	− 37.339990	− 38.252122	− 36.138664
0.45	− 8.697506	− 19.875769	− 35.526732	− 54.436428	− 74.877888	− 95.019092
0.5	0	0	0	0	0	0
0.55	8.697506	19.875769	35.526732	54.436428	74.877888	95.019092
0.6	13.119534	23.725913	32.456799	37.339990	38.252122	36.138664
0.65	12.794482	17.025615	17.078258	14.579929	11.273252	8.172582
0.7	9.950052	9.560950	7.100163	4.601562	2.751791	1.561788
0.75	6.717201	4.663426	2.588410	1.280245	0.590657	0.259959
0.8	4.096495	2.040226	0.835739	0.308672	0.106784	0.035284
0.85	2.274304	0.784115	0.226182	0.059072	0.014458	0.003379
0.9	1.110491	0.240689	0.043903	0.007248	0.001120	0.0001652
0.95	0.406804	0.042170	0.003669	0.000288	0.0000212	0.00000148
1.	0	0	0	0	0	0

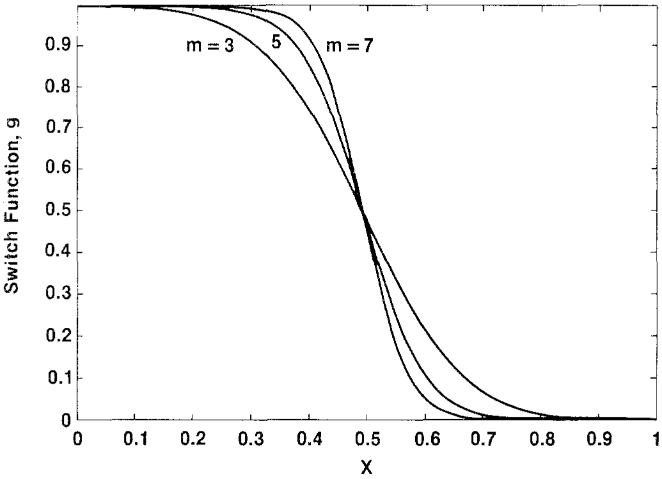

Fig. 2. A power weighted switch function, g, vs x for $m = 3$, 5, and 7.

a smooth behavior near the ends of the interval, the highly nonlinear behavior near the midpoint prevents them from being suitable for the entire interval.

The good features of the low-m and high-m switching functions were combined by using the following power-weighted function:

$$g = g_1 = W_1/(W_1 + W_2)$$

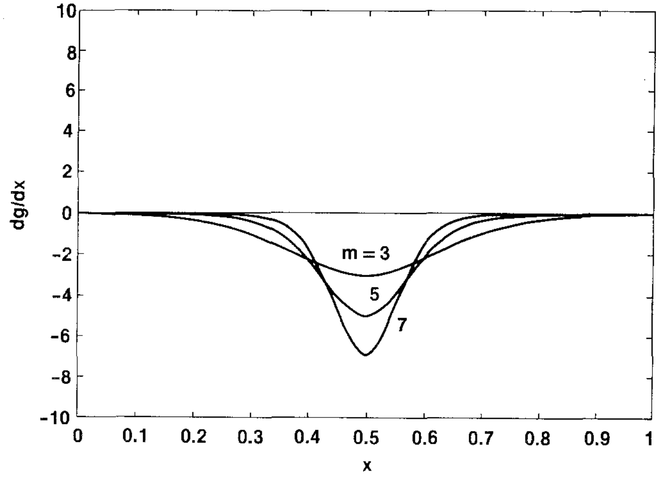

Fig. 3. First derivative of a power weighted switch function vs x for $m = 3$, 5, 7.

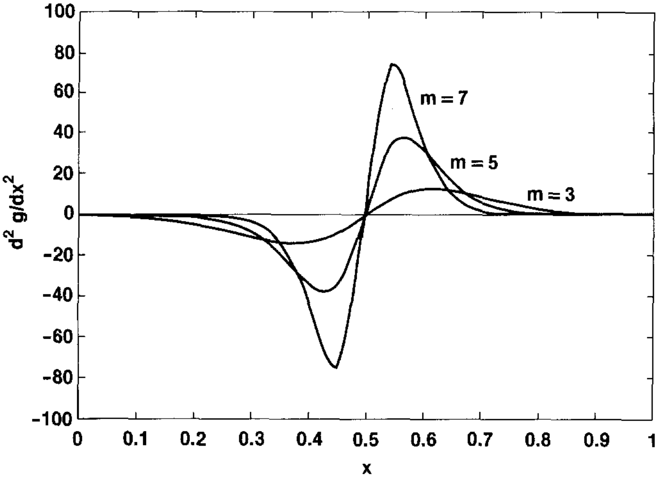

Fig. 4. Second derivative of a power weighted switch function vs x for $m = 3$, 5, and 7.

and

$$1 - g = g_2 = W_2/(W_1 + W_2) \tag{14}$$

where

$$W_1 = (h_1/h_{12})^{m_1}/(1 + c_1 h_1/h_{12})^{m_1 - n}$$

and

$$W_2 = (h_2/h_{12})^{m_2}/(1 + c_2 h_2/h_{12})^{m_2 - n} \tag{15}$$

with h_1 and h_2 given by $h_1 = s_2 - s$ and $h_2 = s - s_1$. Here $h_{12} = h_1 + h_2 = s_2 - s_1$, and n is a third exponent with value near unity. If c_1 and c_2 are chosen to be large, W_1 will be nearly proportional to h_1^n, and W_2 will be nearly proportional to h_2^n, except near the ends of the interval, as $h_1 \to 0$ or $h_2 \to 0$; there W_1 becomes proportional to $h_1^{m_1}$ or W_1 to $h_2^{m_2}$, respectively. Details in regard to derivatives are to be found in Appendix A. The switch function studied in the ensuing treatment is as given by Eqs. (14) and (15). A tentative selection of the parameters $m_1 = 5$, $m_2 = 6$, $n = 1$, $c_1 = 7.25$, and $c_2 = 3.75$ in an application to steam is explained later in Section 10.

5. DISTANCE FROM THE CRITICAL POINT

Up to this point, no definition has been given for distance from the critical point, even though a quantity s has been referred to as a "distance" variable. One very natural choice made by Chapela and Rowlinson [1] was to use the r of the parametric variables r and θ of the scaled equation. They are related to the physical variables T and ρ by

$$\Delta T^* = (T - T_c)/T_c = (1 - b^2\theta^2)r \tag{16}$$

and

$$\Delta\rho^* = (\rho - \rho_c)/\rho_c = k\theta r^{\beta} \tag{17}$$

In practice, however, the range in T, ρ space where the scaled equation applies is not bounded by a contour of constant r, but extends to larger r values as $\theta \to 0$. Thus, it seemed advisable to make a more flexible choice of the distance variable s, such as

$$s = \left[(\Delta T^*)^2 + C(\Delta\rho^*)^2\right]^q \tag{18}$$

with C and q as parameters to be chosen. Small values for q lead to smaller rates of change of the switch function g versus physical variables at larger values of s. This moderates some of the effects of large derivatives in the larger-distance portions of the switching region. The parameter C provides a means for changing contours of equal s from circular ($C = 1$) to oval shapes, increasing flexibility.

A further adjustment,

$$s = \left[(\Delta T^*)^2/(1 + B\Delta T^*) + C(\Delta\rho^*)^2\right]^q \tag{19}$$

was introduced to permit the contours to be displaced upward in the supercritical region to better resemble the shape of the region of validity of the scaled formulation. This is illustrated in Fig. 5, where contours are shown by solid lines for $s = 0.15$, 0.2, and 0.25, with B as 40 and C as 0.01, and with $q = 1/4$. Dotted curves are shown for $s = 0.125$, 0.15, 0.175, and 0.20, with B changed to 65 and C to 0.015. A trapezoidal region is shown corresponding to a similar area shown by Levelt Sengers [3] for which data for steam had been used in obtaining parameters in a scaled formulation [2]. The second choice of B and C gives contours which approach the shape of the scaling region. This function was used for the initial part of the work reported here.

In the later part of the work, further adjustments were made to permit the switching region to be asymmetric in the density $\Delta\rho^*$:

$$s = \left[(\Delta T^*)^2/(1 + B\Delta T^*)^2 + C(\Delta\rho^*)^2/(1 + D\Delta\rho^*)\right]^q \tag{20}$$

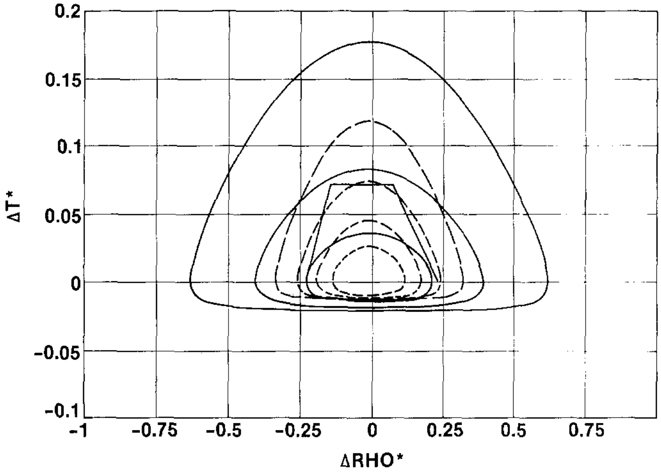

Fig. 5. Contours for distance from the critical point with $B = 40$, $C = 0.01$, s from 0.15 to 0.25 for solid curves; $B = 65$, $C = 0.015$, s from 0.125 to 0.2 for dashed curves. Quadrilateral shows area in which scaled equation was fitted for H_2O.

The distance function actually used was a refinement of (20) containing an even larger number of adjustable parameters. We refer to Appendix B for the form of this distance function. This appendix also contains a simple procedure for selecting values for B, C, and D. In addition, the appropriate derivatives of the more general distance function are given, as required for the calculation of thermodynamic functions. The derivatives of the distance function (19) and (20) are included as special cases of the more general form (B4).

6. AN APPLICATION TO STEAM

It has appeared appropriate to apply the preceding relations to some actual substance as a useful example. A substance for which an accurate classical equation and an accurate scaled equation are already available is steam. For the classical representation, that of Pollak [6, 7] is used. A small change is made with regard to some of Pollak's constants, namely, to introduce new ideal gas properties for water [8]. Near the critical point, the properties have been obtained from the scaled fundamental equation for the critical region of steam of Levelt Sengers [3], based on the so-called restricted linear model of scaling. Two sets of constants were presented in that paper, a "Set G," given three years earlier, and a more recently chosen "Set K," differing only in the analytic temperature dependence of the free energy, set G fitting better at the higher temperatures, and set K better at the lower temperatures.

7. CLASSICAL OR ANALYTIC EQUATION

In the present updating of Pollak's ideal gas constants, the Helmholtz free energy A^0 is represented by

$$-A^0/RT = \left(a_1^0\tau + a_2^0\right)\ln\tau - \sum_{j=3}^{18} a_j^0\tau^{(K+3-j)} \qquad (21)$$

where $\tau = 273.16/T$, with T as the Kelvin temperature. With the revised constants presented here, the value $K = 3$ is used, whereas $K = 1$ if Pollak's constants are used. The coefficients a_j^0 are listed in Table IV. Pollak represented the contribution to the Helmholtz free energy due to equation of state or "real gas" effects using 41 constants. He based his data fit on accepted vapor pressures, with densities and enthalpies at saturation from the International Skeleton Tables, as well as a selection of best P-V-T data.

Table IV. Coefficients a_j^0 Used in Representing the Helmholtz Free Energy for the Ideal Gas; Eq. 20

j	a_j^0
1	$-7.222972258 \cdot 10^0$
2	$-1.99662682 \cdot 10^1$
3	$0.237182038 \cdot 10^{-1}$
4	$-0.811809877 \cdot 10^0$
5	$0.32761657 \cdot 10^0$
6	$2.551804122 \cdot 10^0$
7	$1.17829037 \cdot 10^1$
8	$-3.418592855 \cdot 10^0$
9	$0.9733505265 \cdot 10^0$
10	$-0.2295994604 \cdot 10^0$
11	$0.424758157 \cdot 10^{-1}$
12	$-6.016196693 \cdot 10^{-3}$
13	$6.408636724 \cdot 10^{-4}$
14	$-5.021850753 \cdot 10^{-5}$
15	$2.797503787 \cdot 10^{-6}$
16	$-1.045270809 \cdot 10^{-7}$
17	$2.342344143 \cdot 10^{-9}$
18	$-2.373850853 \cdot 10^{-11}$

Table V. Coefficients a_j and Exponents r_j and t_j of the Canonical Equation of State, Eq. (21)

j	a_j	r_j	t_j
1	$0.4207954763 \cdot 10^1$	1	1
2	$-0.3924884203 \cdot 10^2$	1	2
3	$0.2565923808 \cdot 10^2$	1	3
4	$-0.7837989290 \cdot 10^1$	1	4
5	$0.2201928225 \cdot 10^1$	1	6
6	$-0.1385999869 \cdot 10^0$	1	9
7	$0.3744815486 \cdot 10^1$	2	0
8	$-0.3465071973 \cdot 10^2$	2	2
9	$-0.8425527047 \cdot 10^1$	2	4
10	$-0.9901368699 \cdot 10^1$	3	0
11	$0.1401964088 \cdot 10^3$	3	2
12	$0.1713603120 \cdot 10^2$	4	0
13	$-0.3746614177 \cdot 10^2$	4	1
14	$-0.1159673854 \cdot 10^3$	4	2
15	$-0.1001408944 \cdot 10^2$	5	0
16	$0.3855720938 \cdot 10^2$	5	1
17	$0.1399466356 \cdot 10^2$	5	2
18	$0.1236023923 \cdot 10^2$	7	3
19	$-0.4211642421 \cdot 10^1$	9	3
20	$0.1714623344 \cdot 10^1$	9	5
21	$-0.3840140968 \cdot 10^1$	10	1
22	$0.2325085982 \cdot 10^1$	11	1
23	$-0.2964092990 \cdot 10^1$	12	5
24	$0.1334760540 \cdot 10^1$	14	5
25	$0.3481083585 \cdot 10^1$	1	2
26	$-0.2903770597 \cdot 10^3$	1	5
27	$0.5519480260 \cdot 10^3$	1	6
28	$-0.3736712149 \cdot 10^3$	1	7
29	$-0.1304997844 \cdot 10^4$	2	5
30	$0.8812436076 \cdot 10^4$	2	6
31	$-0.1236192869 \cdot 10^5$	2	7
32	$0.3483212648 \cdot 10^4$	3	2
33	$-0.5346445782 \cdot 10^5$	3	3
34	$0.3230718337 \cdot 10^6$	3	4
35	$-0.9586042785 \cdot 10^6$	3	5
36	$0.1390137766 \cdot 10^7$	3	6
37	$-0.7876922444 \cdot 10^6$	3	7
38	$-0.7696132536 \cdot 10^4$	4	5
39	$0.5188648733 \cdot 10^5$	4	6
40	$-0.7907132902 \cdot 10^5$	4	7

The contribution to free energy due to "real gas" effects is indicated by

$$(-A/RT)-(-A^0/RT)$$

$$= -\sum_{j=1}^{24} a_j\delta^{r_j}\tau^{t_j} - \exp(-a\delta^2)\sum_{j=25}^{40} a_j\delta^{r_j}\tau^{t_j} - \ln(\delta/\delta_{Tr}) \qquad (22)$$

The variable δ here is numerically equal to the density when given in g/cm^3. The constants a_j, r_j, and t_j are listed in Table V, and are as given by Pollak [6] in his Table 3. The coefficient a in the exponential remains 17.5, and δ_{Tr}, numerically the "density" of the liquid at the triple point, at 0.99977602. In various calculations, the relation $\delta = \rho W/V_0$ has been used, where the density ρ was in "ideal" Amagat units ($\rho = V_0/V$). V_0 is the volume of one mole of ideal gas at standard conditions, or 22,413.83 cm^3. W, the molecular weight of the isotopic mixture, was taken as 18.01555, nearly 0.002% above current estimates so as to retain the value Pollak used for the gas constant, $R = 0.461513\ \mathrm{J \cdot g^{-1} \cdot K^{-1}}$.

8. SCALED EQUATION

As mentioned with regard to earlier work [1], the physical variables temperature T and density ρ are represented by

$$T = T_c\left[1 + (1 - b^2\theta^2)r\right]$$

and

$$\rho = \rho_c\left[1 + k\theta r^{\beta}\right] \qquad (23)$$

where r and θ are parametric variables somewhat like polar coordinates, useful in scaled representations by the restricted linear model. The formulation for the reduced free energy density, as

$$A^* = A_0^*(T^*) + \rho^*\mu^*(\rho_c, T^*) + A_{\mathrm{anom}}^* \qquad (24)$$

is in units of VP_c. Here $A_0^*(T^*)$ and $\mu^*(\rho_c, T^*)$ are regular functions of T^*, while A_{anom}^* contains the critical anomalies. Conversion with $P_0V_0/RT_0 = 1$ as for an ideal gas leads to

$$-A/RT = -\frac{P_c}{P_0}\frac{T_0}{T}\frac{A^*}{\rho} \qquad (25)$$

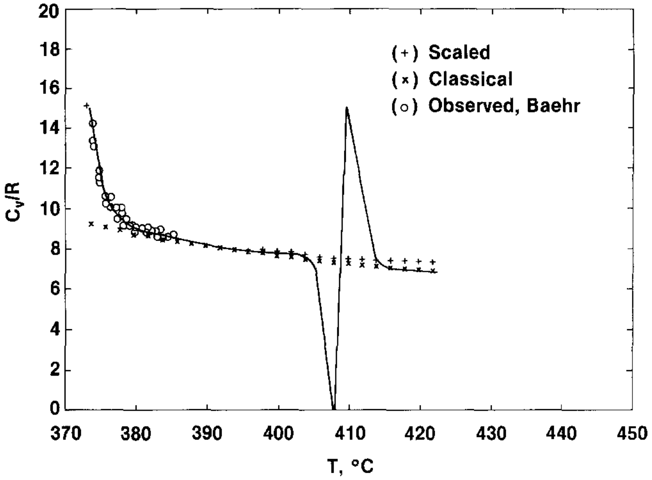

Fig. 6. C_v/R for steam at 3.25 $cm^3 \cdot g^{-1}$, near critical density, by Pollak (classical), Levelt Sengers (scaled), Set K, and switch function with $m_1 = m_2 = 6$, $n = 1$, $c_1 = c_2 = 0$. "Distance" with $B = 65$, $C = 0.015$, $D = 0$. Values from Baehr are for 3.223 $cm^3 \cdot g^{-1}$.

where P_0 is a pressure of 1 atm and T_0 is 273.15 K, as for standard conditions, $\rho = V_0/V$ is the ideal Amagat density, and A is the molar free energy. Additional details, including the different background constants for "Set G" and "Set K" of Levelt Sengers [3] may be found in Appendix C.

9. BEHAVIOR IN THE SWITCH REGION

A graphical presentation of computed estimates for C_v/R near the critical density and involving a switching region between $s_1 = 0.15$ and $s_2 = 0.175$ or between 674 K and 692 K (401°C and 419°C) is shown in Fig. 6 using the "Set K" constants and the switch function of Eqs. (14) and (15) with $m_1 = m_2 = 6$, $n = 1$, and $c_1 = c_2 = 0$. Some data of Baehr and Schomächer are also shown [9]. The very large "overshoots" of the blended C_v are clearly due to the large values of the second derivative of the switch function. By increasing the constants c_1 and c_2 of Eqs. (14) and (15) to the value 6, as shown in Fig. 7, considerable improvement is obtained, but the behavior in the switching region is still unsatisfactory. Further improvement can be made by modifications of the free energy surfaces so as to bring them closer together.

Figure 8 shows plots of an Arrhenius type for the difference $(-A/RT)_{\text{scaled}} - (-A/RT)_{\text{classical}}$ versus $1/T$, using the "Set K" constants for the scaled formulation. When these were compared with diagram (c) of Fig.

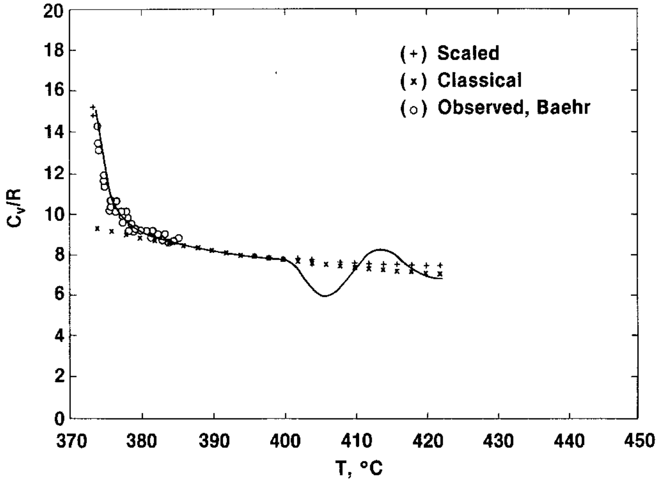

Fig. 7. C_v/R for steam at 3.25 $cm^3 \cdot g^{-1}$, near critical density by Pollak (classical), Levelt Sengers (scaled), Set K, and switch function with $m_1 = m_2 = 6$, $n = 1$, $c_1 = c_2 = 6$. "Distance" as for Fig. 6. Values from Baehr are for 3.223 $cm^3 \cdot g^{-1}$.

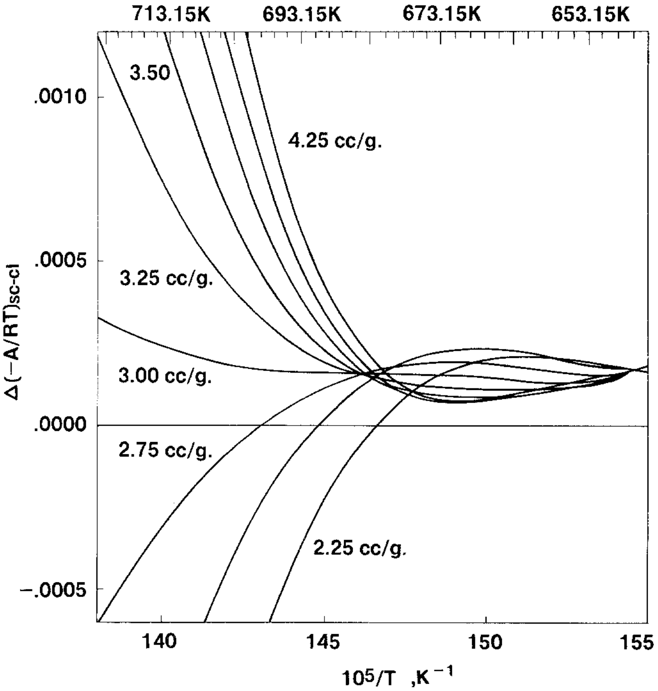

Fig. 8. Arrhenius type plot of $(-A/RT)_{\text{scaled}} - (-A/RT)_{\text{classical}}$ for the scaled Set K constants of Levelt Sengers and the classical of Pollak for water.

1, it was seen that not all are in the favored relative position of near tangency with the zero axis, in the region 3.5 to 4 $cm^3 \cdot g^{-1}$ and 653 to 673 K.

In the case of similar curves using the "Set G" constants of ref. [3], shown in Fig. 9 for several isochores, the general behavior is more acceptable according to the discussion given in regard to diagram (c) of Fig. 1, provided the zero axis can be suitably shifted upward. To accomplish this, there is a need for a revised choice of integration constants in regard to energy and entropy, in the fit of the scaling representation. In the present instance, the revision has been taken as a parallel shift of the zero axis to be above the curves, or adjacent to their convex side, in the region of the expected switching above the critical temperature. It can be seen that changes in the constants μ_0^* and μ_1^* in the power series expansion of $\mu^*(\rho_c^*, T^*)$ would be consistent with a preservation of character of the Arrhenius diagram equivalent to changing the position and slope of the

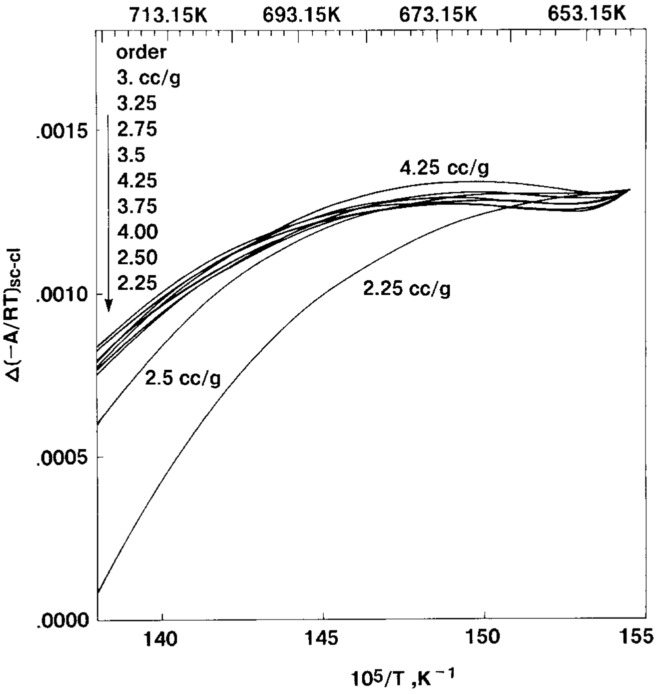

Fig. 9. Arrhenius type plot of $(-A/RT)_{\text{scaled}} - (-A/RT)_{\text{classical}}$ for the scaled Set G constants of Levelt Sengers and the classical of Pollak for water.

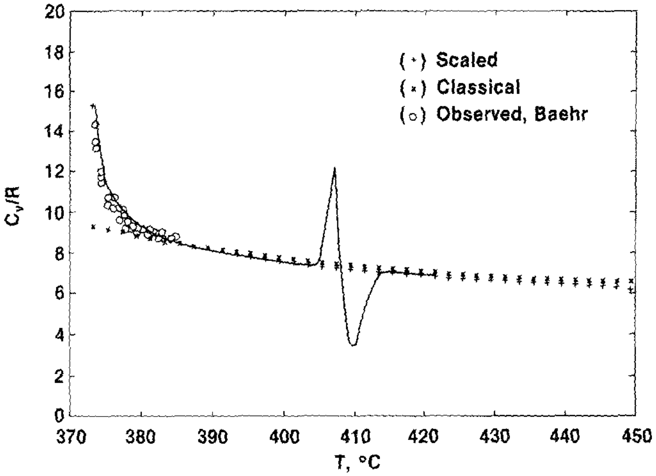

Fig. 10. C_v/R for steam at 3.25 $\text{cm}^3 \cdot \text{g}^{-1}$, near critical density, by Pollak (classical), Levelt Sengers (scaled), Set G, reset to $\mu_0 = -11.2982$, $\mu_1 = -34.0192$, switch function with $m_1 = m_2 = 6$, $n = 1$, $c_1 = c_2 = 0$. "Distance" and observed values as for Fig. 6.

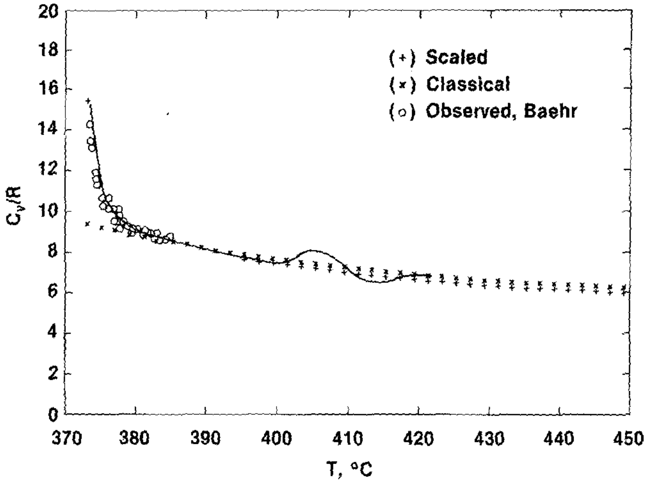

Fig. 11. C_v/R for steam at 3.25 $\text{cm}^3 \cdot \text{g}^{-1}$, near critical density, by Pollak (classical), Levelt Sengers (scaled), etc., as in Fig. 10, except switch function is with $m_1 = m_2 = 6$, $n = 1$, $c_1 = c_2 = 6$.

zero axis. Explicitly, the change in $-A/RT$ is

$$\delta(-A/RT) = -\frac{P_c V_c T_0}{P_0 V_0 T_c}\{\delta\mu_1^* + (\delta\mu_0^* - \delta\mu_1^*)T_c/T\} \tag{26}$$

If no change of slope is to be made, then $\delta\mu_0^* - \delta\mu_1^* = 0$. In the present instance, an addition of 0.0058 to both μ_0^* and μ_1^*, to give $\mu_0^* = -11.2892$ and $\mu_1^* = -34.0192$, is found to subtract 0.00132 from $(-A/RT)_{\text{scaled}}$. The constant $P_c V_c T_0 / P_0 V_0 T_c$ in (26), which is Z_c, the compressibility factor at the critical point, equals 0.2276. With this change, the zero axis for the $\Delta(-A/RT)_{sc\text{-}cl}$ plot is moved to a more favorable position for near tangency for temperatures somewhat above the critical.

With these adjusted values for μ_0 and μ_1 of the "Set G" constants, the computed values for C_v/R are as shown in Fig. 10 for the case of $m_1 = m_1 = 6$, $n = 1$, and $c_1 = c_1 = 0$, a considerable improvement over that in Fig. 6, The shift to $c_1 = c_2 = 6$ gives the curves of Fig. 11, where the maximum "overshoots" of C_v begin to approach the experimental noise.

10. IMPROVEMENT OF SWITCHING PARAMETERS

Further improvement of the switching process can be achieved by adjusting the parameters in the switch function so as to closely match the empirical estimates for an "ideal" blend function, as obtained from graphical interpolations between the two free energy surfaces along a number of isochores. These graphical interpolations also determine empirical upper and lower bounds for the distance function, for which a refined representation is developed. The procedure is as follows. In Figs. 12–17, values for $\Delta(-A/RT)_{sc\text{-}cl}$ are shown versus $10^5/T$ for various isochores for specific volumes from 4.0 to 2.75 $\text{cm}^3 \cdot \text{g}^{-1}$. The free energy surfaces are those of Pollak, with revised ideal-gas properties, and the scaled surface "G" with revised values of μ_0^*, μ_1^*. For the free energy in the switch region, a behavior as indicated by the heavy curves in these figures is desired. This curve is intermediate between the two free energy surfaces, and its curvature is also intermediate. It should therefore yield intermediate C_v/R and A/RT values; the internal energy, however, cannot be expected to be intermediate.

On any isochore, the departure of the heavy line from the zero axis at a specified temperature, divided by the distance of the two surfaces at that temperature, provides an estimate of the local value of the desired switch function. Values obtained in this way for the empirical switch function along the four isochores with specific volumes of 2.75, 3.00, 3.25, and 3.50

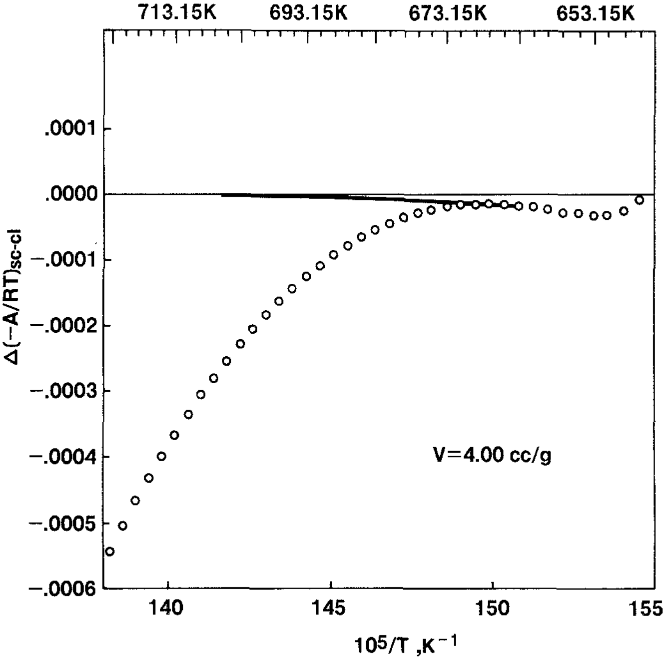

Fig. 12. Arrhenius type plot of $(-A/RT)_{\text{scaled}} - (-A/RT)_{\text{classical}}$ for water at 4.00 $\mathrm{cm}^3 \cdot \mathrm{g}^{-1}$. Scaled is with adjusted integration constants for Set G of Levelt Sengers, classical by Pollak. A curve switching from scaled somewhat below 670 K to classical near 720 K is shown.

$\mathrm{cm}^3 \cdot \mathrm{g}^{-1}$, respectively, and plotted in Fig. 18, versus the distance variable $x = (s - s_1)/(s_2 - s_1)$. The distance function used is that given by Eq. (B4) in Appendix B; the parameter values used are given in Fig. B2. The choices of the inner and outer boundaries of the switching region were made basically in accordance with those in Figs. 14–17. Near the critical density, the switching region extends from 663 K to 721 K. For the outer boundary, the density limits were about 262 and 565 amagat. For the inner boundary, the lower temperature limit was about 637 K and the density limits at the critical temperature were about 313 and 504 amagat. The outer boundary extends beyond the range of validity of the scaled equation—the small discrepancies introduced by the increased difference between the two free energy surfaces near the outer boundary are outweighed by the reduction in size of the derivatives resulting from extending the switching range.

With the newly adjusted switching function parameters and the modified "Set G" constants, the blend values for C_v/R near the critical isochore are considerably improved, as may be seen from Fig. 19, which shows no

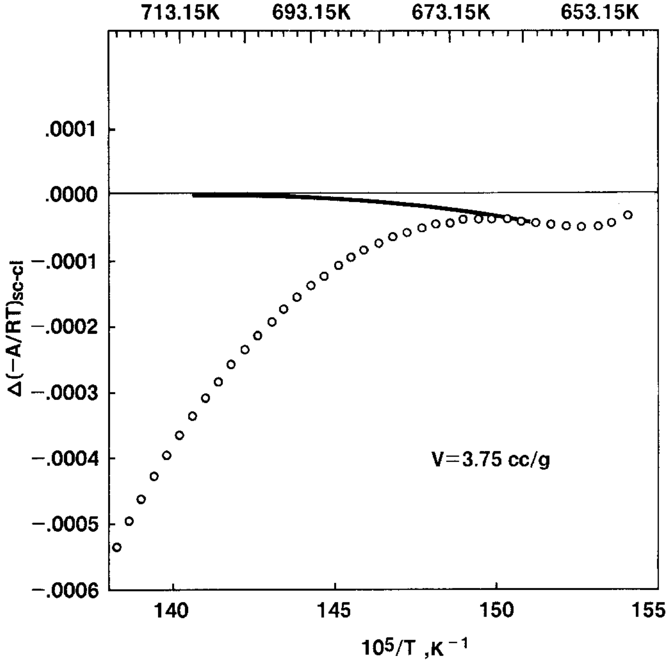

Fig. 13. Same as Fig. 12 except $V = 3.75\ \mathrm{cm}^3 \cdot \mathrm{g}^{-1}$.

evident departure from desired behavior. The values follow the scaled formulation in agreeing with C_v data of Baehr and Schomäcker above the critical temperature; they then have a smooth crossover in the region 390° to 450°C, roughly; and, lastly, they proceed upward with the classical values of Pollak. It is, of course, necessarily true that the free energy function progresses simply and smoothly between the scaled and classical formulation values in crossing the switching region. This is not necessarily achieved for all other functions, as has been pointed out. In connection with Fig. 1 it was shown that the internal energy will not be intermediate between scaled and classical when intermediacy is obtained for both free energy A and heat capacity C_v. The behavior of the internal energy along the 3.25 $\mathrm{cm}^3 \cdot \mathrm{g}^{-1}$ isochore as indicated with the present switching adjustment is shown in Fig. 20, where percent deviations from the classical are shown for both scaled and blend values. The blend values are above both scaled and classical throughout the switching region, with no excursion whatever into the intermediate value region, just as predicted. The magnitude of the discrepancy is rather small, however, namely, less than 0.02% at the maximum.

The improvement in fit of C_v/R data in progresssing from the original

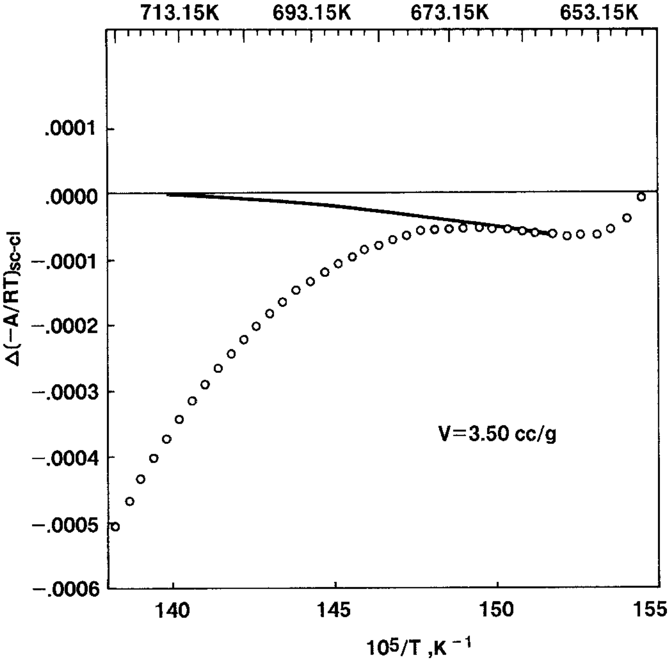

Fig. 14. Same as Fig. 12 except $V = 3.50\ \mathrm{cm}^3 \cdot \mathrm{g}^{-1}$.

"Set K" constants of Fig. 6 to the "Set G" constants for Fig. 19 can scarcely end the task of studying the switching problem. Other thermodynamic properties also exist which pertain to derivatives of $-A/RT$ with respect to density. These also must be examined in regard to desirable behavior.

In Fig. 21 are shown values of the dimensionless quantity $d\ln P/d\ln\rho$, related to the compressibility, for the scaled, classical, and blend formulations with the same parameters as used for Fig. 19. The curves here follow the computed "blend" values obtained for several isotherms. The separately plotted points show the corresponding scaled and classical values, where different, at the several densities of the calculations. It is seen that blend values not intermediate between scaled and classical may be given by the calculation. It is obvious that the relationships in regard to first and second derivatives with respect to temperature as pointed out in connection with the discussion of Fig. 1 must also apply qualitatively in regard to first and second derivatives with respect to density.

As a practical detail, then, the idea might be considered as to whether the effort to attain nearly perfect behavior of C_v/R displayed in Fig. 19

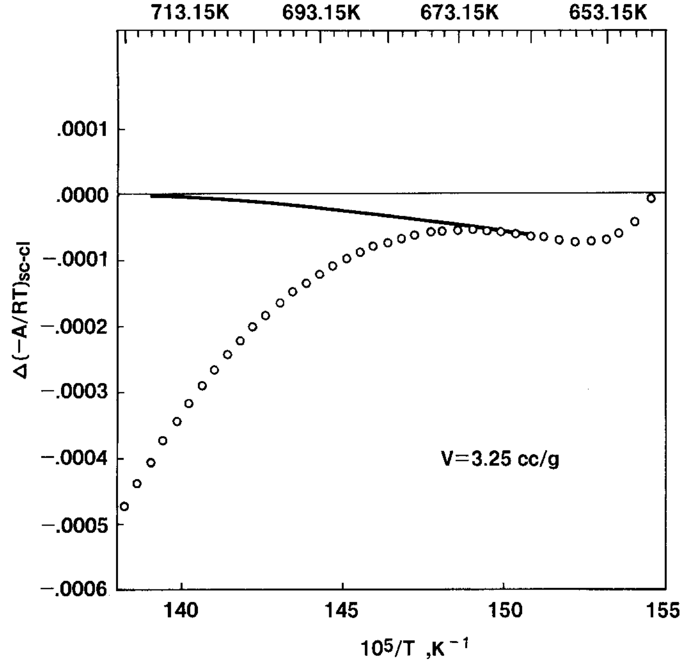

Fig. 15. Same as Fig. 12 except $V = 3.25\ \text{cm}^3 \cdot \text{g}^{-1}$.

may have been carried to a point beyond the optimum for an overall satisfactory representation of thermodynamic behavior in the blend region. Thus, some relaxation of the requirements for C_v/R may permit further useful improvement for the density derivatives. This may be a consideration for later study.

Some impressions as to problems involved in attempting to improve density dependences may be gained from a suitable graphical presentation. In Fig. 22 some curves are shown for $\delta(-A/RT)_{sc\text{-}cl}$ for several values of temperature for specific volumes from 2 to 5.25 $\text{cm}^3 \cdot \text{g}^{-1}$, as obtained from a computer print-out using the same modification of scaling constants as used in regard to Figs. 19–21, namely, "Set G," with μ_1 and μ_2 as readjusted. It is perhaps easiest to consider the switching task as one of finding replacement curves that would follow the curves as shown in a limited region above and below the value for the critical volume[2] of 3.098

---

[2] This value was recently given by Levelt Sengers et al. [10]; alternatively, it is about 3.10. Other values include 3.08279 (scaled, Levelt Sengers) and 3.155 (classical, Pollak).

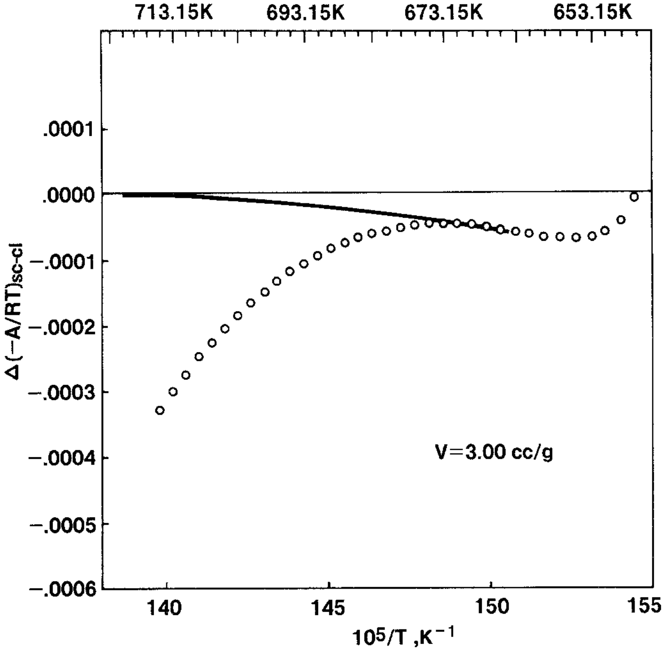

Fig. 16. Same as Fig. 12 except $V = 3.00\ \mathrm{cm^3 \cdot g^{-1}}$.

$\mathrm{cm^3 \cdot g^{-1}}$, but with all going to the zero ordinate axis outside the critical region. In the general vicinity of the critical volume, the replacement or blend curves far above the critical temperature would be near the (horizontal) zero axis since the "blend" would be nearly or quite exactly identical with the classical values. (Thus it should be for the 450°C curve, which is beyond the range for simple scaling.) For isotherms only slightly above the critical temperature, the curves would "sag" appreciably below the zero axis in the critical volume region, but approach the axis at specific volumes both considerably below and also considerably above the critical volume. This may suggest that a very judicious choice of regions in which the switching occurs might fulfill the need for smoothly varying curves fairing into the zero axis in leaving the critical region. Allowing for a possibility for some small readjustment in μ_0 and μ_1, it may appear that an acceptable answer to switching requirements should be possible. The question of whether such a formulation would be reconcilable with previously adopted global choices for types of switching function and "distance contour" functions might require detailed analysis.

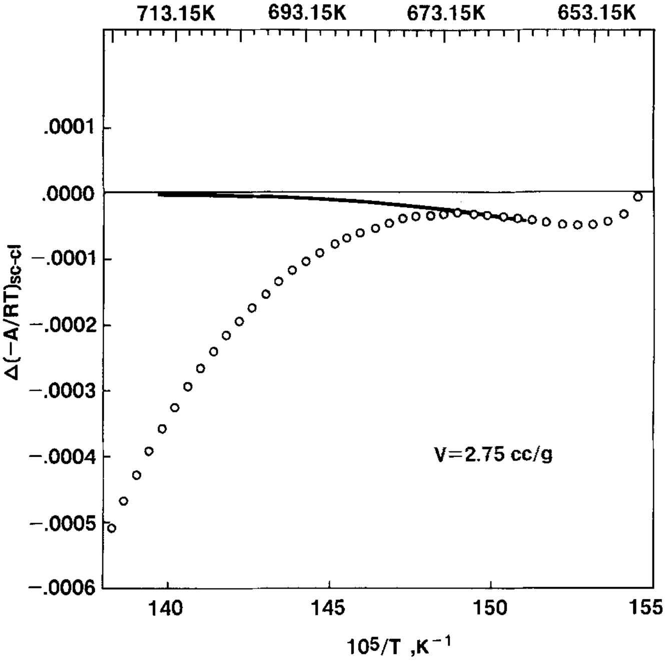

Fig. 17. Same as Fig. 12 except $V = 2.75\ \mathrm{cm}^3 \cdot \mathrm{g}^{-1}$.

11. CONCLUDING REMARKS

We have formulated a procedure for producing smoothly changing values for the thermodynamic properties for a substance in an intermediate region between two regions in which distinctly different empirical representations have been obtained. The particular application is made by using a switching function as a changing relative weight in regard to Helmholtz free energies in connecting a scaled equation formulation near the critical point and a classical equation formulation further away. Other related thermodynamic functions follow naturally by differentiation.

The study has included the choice of a usable form of switching function in regard to dependence on "distance" from the critical point. Various steps of generalization are shown in regard to improving an initial prescription for specifying "distance" from the critical point. The aim in this is for the capability of tailoring of the shapes of distance contours to help adjust for local behavior differences in the thermodynamic formulations to be reconciled.

The most striking finding from this investigation is that the simple act of arranging for A, the Helmholtz free energy, in the switching region to be

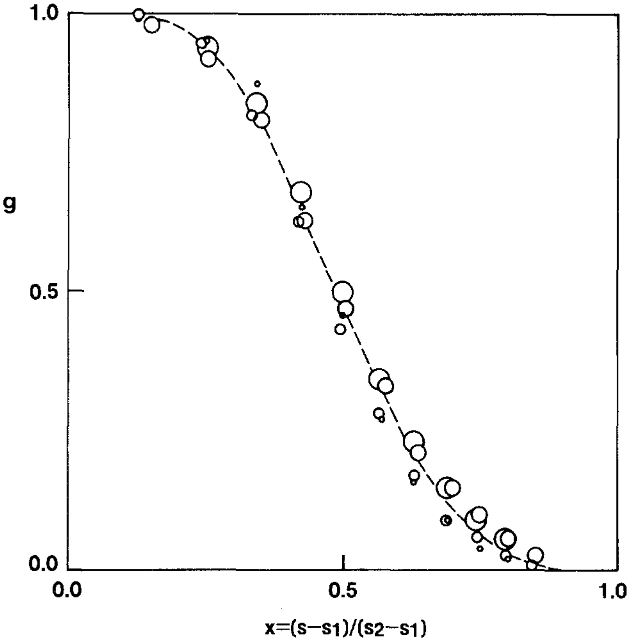

Fig. 18. Suitable switching behavior estimated for water from tangent curves drawn in some Arrhenius plots (∘, 2.75 $cm^3 \cdot g^{-1}$; ○, 3.00 $cm^3 \cdot g^{-1}$; ◯, 3.25 $cm^3 \cdot g^{-1}$; ◯, 3.50 $cm^3 \cdot g^{-1}$)

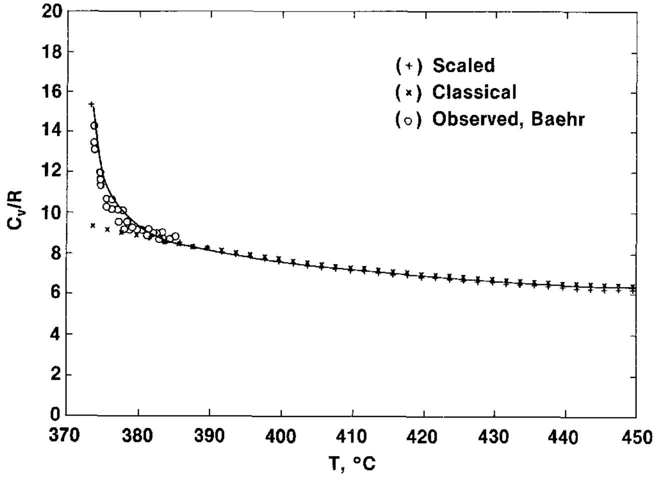

Fig. 19. C_v/R for steam at 3.25 $cm^3 \cdot g^{-1}$, near critical density, by Pollak (classical), Levelt Sengers (scaled), as in Fig. 11, except switch function uses $m_1 = 5$, $m_2 = 6$, $n = 1$, $c_1 = 7.25$, $c_2 = 3.75$. "Distance" with $B = 26.67$, $C = 0.00358$, $E = 1.568$, $G = -57.1$, $H = 300.8$.

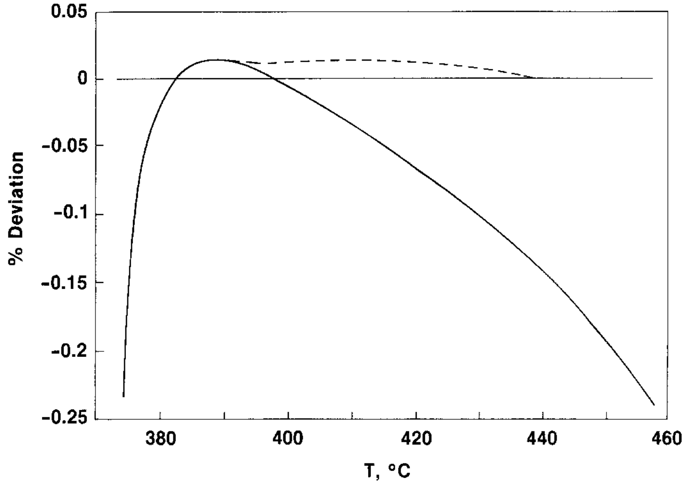

Fig. 20. Comparison of blend internal energy, scaled and classical, at 3.25 $cm^3 \cdot g^{-1}$. Deviation in percent vs classical for scaled (solid line) and blend (dashed line). Parameters are as for Fig. 19.

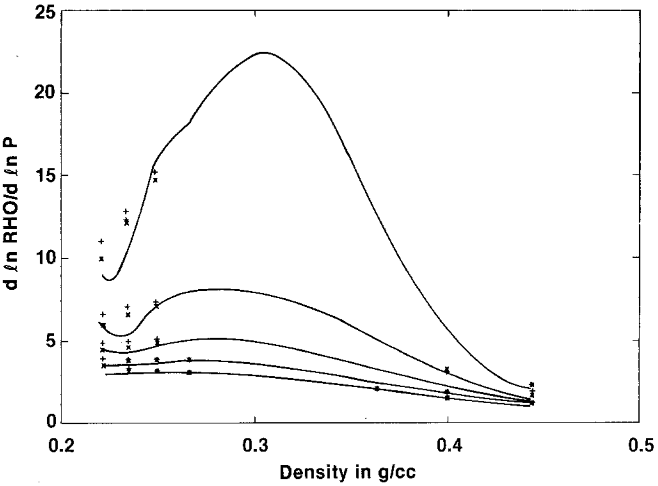

Fig. 21. Comparison of estimates for compressiblity, $d \ln \rho / d \ln P$ or $-(P/V)dV/dP$, for steam. The curves show computed blend values for 380, 390, 400, 410, and 420°C, reading downward on the graph. Points are for scaled (+) and classical (×), where the blend value is more than 1% away from both.

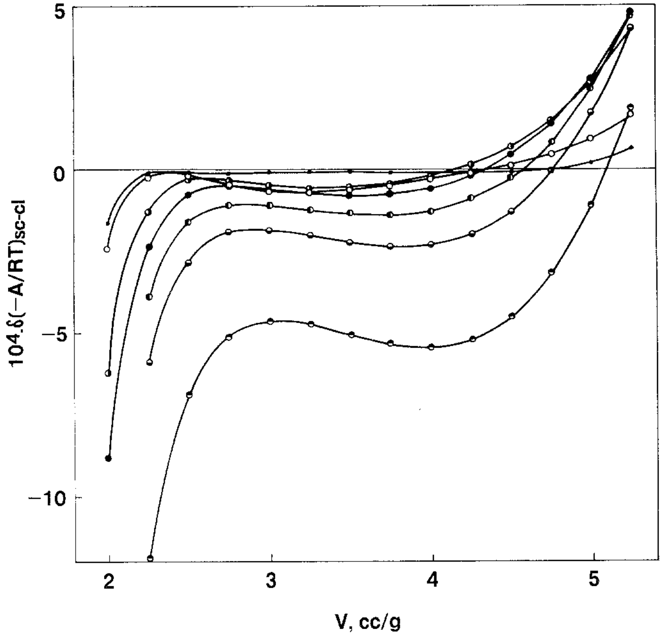

Fig. 22. Behavior of the difference, scaled minus classical, for $-A/RT$ for steam vs volume at several temperatures. Classical values by Pollak, scaled by Levelt Sengers. (Set G except for change of μ_0^* to -11.2892 and μ_1^* to -34.0192.) Temperatures are · 374°C; ○ 380°C; ◑ 400°C; ● 410°C; ◐ 420°C; ◒ 430°C; ◓ 450°C.

between the respective free energy values from the scaled and classical formulations is not sufficient to guarantee a similar condition of intermediacy in the derived functions such as the internal energy U and the specific heat C_v. The finding is in fact even more strongly adverse! From simple graphical considerations it can even be seen that it is fundamentally impossible for such a condition of intermediacy to be obtained simultaneously for both U and C_v. Accordingly, there should be some relaxing of expectations as to what the achievable satisfactory behavior of derived properties would be. The same considerations apply in regard to functions obtained by differentiation with respect to density.

As to conclusions with regard to a desirable form for the switch function, it was found that a beginning assumption that the function might be of a "power weighted" type, Eq. (13), with exponent values of 4 or more in regard to "distance" into the switch region gave no particularly sudden change on entering the region. Raising these exponent values considerably would further improve the smoothness of switching here; however, it causes derivatives of the switch function to become excessively large near the central part of the switching region. It was found that these overly rapid rates of change could be alleviated considerably by some algebraic modifications in the defining equation, by making it more linear in the central part of the region.

On a second topic, "distance" and the shape of "equal distance" contours, it is found that provision can be made for rather extensive adjustability. Some explorations with the objective of controlling derivative behavior by this means have been made, with very moderate success.

In general, a problem with the behavior of derivatives is seen to be always present in the use of a switching function. If there is a region of moderate difference between "scaled" and "classical" formulations, this might become a region for "switching" or "crossover." However, there will be a problem of finding a suitable compromise between having a narrow region for switching, where the two formulations are not greatly different, versus a region broadened in the hope of decreasing the magnitudes of the derivatives of the switch function. If the region is broadened, however, the numerical differences between the two formulations then become large within the region and, though multiplied by smaller switch-function derivatives, may still give very sizable contributions to the derived thermodynamic functions. The best that can be hoped for is a judiciously chosen compromise.

In view of the inherent difficulties in the overall task of "switching," it appears appropriate to place very special emphasis on the need for high quality of agreement between the two formulations throughout the region of "switching" or "crossover." It seems appropriate that such improved agreement might be sought by way of improvement in both scaled and classical formulations in the crossover region.

As to improvements to be made in the scaled formulation, it is admitted that versions of the restricted linear model were the only ones used in the test cases that are here reported on, whereas extended scaling [10] may make a useful improvement permitting closer agreement with data further away from the critical point. It may also improve the slope of the "rectilinear diameter," which had been taken as zero in the present application of the restricted linear model. We would presume that some further adjustment in the analytic background for the scaled formulations might be desirable. The versions of analytic background that were used provided only a linearly dependent contribution to C_v/R versus temperature. One is inclined to speculate that nonzero derivatives of all orders are probably present and would in theory exist since they do exist for the ideal gas, and further contributions would be expected according to classical formulations pertaining to virial effects.

The limitations in the classical equation of state formulation include those inevitably present in attempting to approximate nonclassical critical behavior with functions for which exact fitting in the critical region is impossible. With perhaps from 30 to 60 or more constants used in the classical equations in achieving an approximate global fit to data in both vapor and liquid regions, it may be very difficult to include also a delicate matching of observed behavior in the region just above the critical temperature. Finally, a close linkage between "scaled" and "classical" data correlation activity might be highly desirable to help in arriving at correlations suitably compatible in a convenient switching or crossover region.

ACKNOWLEDGMENTS

The author wishes to thank the National Bureau of Standards and his colleagues for computing arrangements, interest, and advice facilitating his efforts as a guest worker toward completion of this study. In particular, the suggestion of a power-weighted type of switching function and of using direct physical quantities to give a measure of distance from the critical point were essential contributions of Dr. J. M. H. Levelt Sengers, as also was her advice about limitations in extrapolation of the early results of simple scaling. The comments of Lester Haar in serving to supply general insight and awareness of the vulnerability of data fitting processes to systematic observational error are also particularly appreciated.

APPENDIX A: DERIVATIVES OF THE SWITCH FUNCTION

Derivatives of the switch function indicated by Eqs. (14) and (15) are readily obtained. With the general relations of Eq. (13) and with $dh_1/ds = -1$ and $dh_2/ds = 1$, one has

$$dg/ds = -W_2(W_1 + W_2)^{-2}dW_1/dh_1 - W_1(W_1 + W_2)^{-2}dW_2/dh_2 \quad \text{(A1)}$$

and

$$\begin{aligned} d^2g/ds^2 = & -2W_2(W_1 + W_2)^{-3}(dW_1/dh_1)^2 + W_2(W_1 + W_2)^{-2}d^2W_1/dh_1^2 \\ & -2(W_1 - W_2)(W_1 + W_2)^{-3}(dW_2/dh_2)(dW_1/dh_1) \\ & +2W_1(W_1 + W_2)^{-3}(dW_2/dh_2)^2 \\ & -W_1(W_1 + W_2)^{-2}d^2W_2/dh_2^2 \end{aligned} \quad \text{(A2)}$$

In the present special case, the derivatives indicated become

$$\begin{aligned}
dW_1/dh_1 &= W_1h_1^{-1}(m_1 + nc_1h_1/h_{12})/(1 + c_1h_1/h_{12}) \\
d^2W_1/dh_1^2 &= W_1h_1^{-2}\big[m_1(m_1 - 1) + 2m_1(n - 1)c_1h_1/h_{12} \\
&\qquad + n(n - 1)(c_1h_1/h_{12})^2\big]/(1 + c_1h_1/h_{12})^2 \\
dW_2/dh_2 &= W_2h_2^{-1}(m_2 + nc_2h_2/h_{12})/(1 + c_2h_2/h_{12}) \\
d^2W_2/dh_2^2 &= W_2h_2^{-2}\big[m_2(m_2 - 1) + 2m_2(n - 1)c_2h_2/h_{12} \\
&\qquad + n(n - 1)(c_2h_2/h_{12})^2\big]/(1 + c_2h_2/h_{12})^2
\end{aligned} \tag{A3}$$

Equation (14) can also be used with functions of exponential type such as $W_1 = \exp(-c_1\xi)$ and $W_2 = \exp(c_2\xi)$, where

$$\xi = k/x - 1/(1 - x) + \Sigma a_n(x - 1/2)^n \tag{A4}$$

with $x = (s_2 - s)/(s_2 - s_1)$. The coefficients a_n in the indicated polynomial provide flexibility for tailoring the shape of the resulting curve for g. The expression for g in Eq. (14) can also be given as $(1 + W_2/W_1)^{-1}$ or $[1 + \exp(c\xi)]^{-1}$, where $c = c_1 + c_2$. With this use of the exponential, the function g would have the interesting property that all its derivatives with respect to s would be zero at $s = s_1$ and at $s = s_2$. It does not appear likely that the function would be especially inferior to the power weighted function, examined here in considerable detail.

For this exponential type function, the derivatives of interest would involve

$$\frac{dg}{d\xi} = -c\exp(c\xi)\big[1 + \exp(c\xi)\big]^{-2} \tag{A5}$$

and

$$\frac{d^2g}{d\xi^2} = c^2\exp(c\xi)\cdot\big[\exp(c\xi) - 1\big]\big[1 + \exp(c\xi)\big]^{-3} \tag{A6}$$

with also

$$\begin{aligned}
d\xi/dx &= -k/x^2 - 1/(1 - x)^2 + \Sigma na_n(x - 1/2)^{n-1} \\
d^2\xi/dx^2 &= 2k/x^3 - 2/(1 - x)^3 + \Sigma n(n - 1)a_n(x - 1/2)^{n-2}
\end{aligned} \tag{A7}$$

Then as $dx/ds = -(s_2 - s_1)^{-1}$ and $d^2x/ds^2 = 0$, one has

$$\frac{dg}{ds} = -\frac{dg}{d\xi}\frac{d\xi}{dx}(s_2 - s_1)^{-1} \tag{A8}$$

and

$$\frac{d^2g}{ds^2} = \left[\frac{dg}{d\xi}\frac{d^2\xi}{dx^2} + \frac{d^2g}{d\xi^2}\left(\frac{d\xi}{dx}\right)^2\right](s_2 - s_1)^{-2} \tag{A9}$$

APPENDIX B: THE DISTANCE FUNCTION

The selection of suitable values for B, C, and D in Eq. (20) may be quite straightforward if the desired shape of the distance contours is simple and their desired position is known. Reference is made to Fig. B1 to help clarify the procedure. The temperature intercepts of the inner contour $s = s_1$ on the ΔT^* axis are shown as ΔT_H^* above T_c and ΔT_M^* (a negative value) below T_c. The corresponding density intercepts on the $\Delta\rho^*$ axis are shown as $\Delta\rho_H^*$ at a density greater than ρ_c and $\Delta\rho_M^*$ (a negative value) below ρ_c.

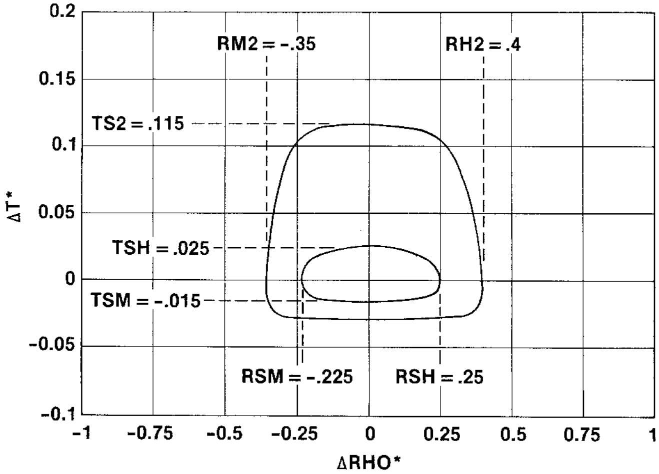

Fig. B1. Contours of "distance" from the critical point. Intercepts on the ΔT^* axis and the Δrho* axis are shown, with $TS2 = 0.115$, $TSH = 0.025$, $TSM = -0.015$, $RSH = 0.25$, $RSM = -0.225$, $RHZ = 0.4$, $RM2 = -0.35$. s_1 and s_2 are 0.14 and 0.24.

The parameters in question are then given by

$$B = -\left(\Delta T_M^{*-1} + \Delta T_H^{*-1}\right), \qquad D = -\left(\Delta \rho_M^{*-1} + \Delta \rho_H^{*-1}\right)$$

and

$$C = \Delta T_H^* \Delta T_M^* / (\Delta \rho_H^* \Delta \rho_M^*) \tag{B1}$$

The value for s_1 is given by $s_1 = y_1^q$, where

$$y_1 = -\Delta T_M^* \Delta T_H^* \tag{B2}$$

Similar relations might be used in regard to the $s = s_2$ contour, for which the temperature intercept on the ΔT^* axis above T_c is shown in Fig. B1 as ΔT_{H2}^*. The value for s_2 is then given by $s_2 = y_2^q$, with

$$y_2 = \Delta T_{H2}^* / \left(B + \Delta T_{H2}^{*-1}\right) \tag{B3}$$

A somewhat more generalized form than Eq. (20) is shown here as Eq. (B4):

$$\begin{aligned} s = \Big[&(\Delta T^*)^2(1 + F)(1 + B\Delta T^*)^{-1} \\ &+ C(\Delta\rho^*)^2(1 + E + A\Delta T^*)(1 + D\Delta\rho^*)^{-1}\Big]^q \end{aligned} \tag{B4}$$

with

$$A = \sum_1^4 a_n \Delta\rho^{*n}, \qquad E = \sum_1^4 e_n \Delta\rho^{*n}$$

and

$$F = \sum_1^4 f_n \Delta\rho^{*n}$$

The numerous internal parameters now included provide considerable flexibility in adjusting the switching region. The choice of method of selecting suitable parameter values is to be left quite open for the present, however. It may possibly be expeditious for some of the parameters to be chosen separately, perhaps as zero, according to possible convenience, and for the remaining ones to be adjusted carefully as circumstances permit or dictate. One particular set of constants leading to the contour plots shown

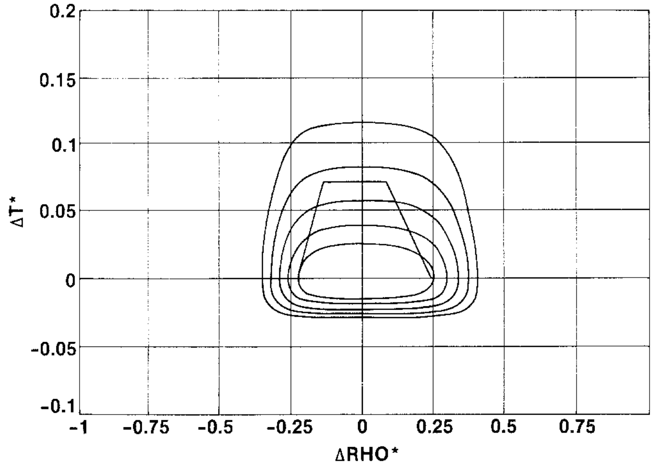

Fig. B2. Contours of "distance" from the critical for the case used here for steam: $B = 26.67$, $C = 0.00358$, $D = 0$, $e(i)$ as 1.568, 0, -57.1, and 300.8; $a(i)$ as 0, $f(i)$ as 0. This case applies to Figs. 19–21. $m_1 = 5$, $m_2 = 6$, $n = 1$, $c_1 = 7.25$, and $c_2 = 3.75$ were used.

in Fig. B2 is the same as used in calculations of thermodynamic quantities leading to the graphs of Figs. 19–21. Suitable logical statements in the computer program may help avoid problems from s in regions other than the desired one for switching.

With a relation of the $s = y^q$ type occurring in Eqs. (18)–(20) and the more general Eq. (B4), the evaluation of Eq. (12) requires derivatives for which the following relations are of use:

$$T\partial s/\partial T = qy^{q-1}T\partial y/\partial T = qs^{1-1/q}Ty_T$$

$$T^2\partial^2 s/\partial T^2 = q(q-1)y^{q-2}T^2(\partial y/\partial T)^2 + qy^{q-1}T^2\partial^2 y/\partial T^2$$

$$= q(q-1)s^{1-2/q}T^2 y_T^2 + qs^{1-1/q}T^2 y_{TT}$$

$$\rho\partial s/\partial\rho = qy^{q-1}\rho\partial y/\partial\rho = qs^{1-1/q}\rho y_\rho$$

$$\rho^2\partial^2 s/\partial\rho^2 = q(q-1)y^{q-2}\rho^2(\partial y/\partial\rho)^2 + qy^{q-1}\rho^2\partial^2 y/\partial\rho^2$$

$$= q(q-1)s^{1-2/q}\rho^2 y_\rho^2 + qx^{1-1/q}\rho^2 y_{\rho\rho}$$

and

$$T\rho\partial^2 s/\partial T\partial\rho = q(q-1)s^{1-2/q}T\rho y_T y_\rho + qs^{1-1/q}T\rho y_{T\rho} \qquad \text{(B5)}$$

The required derivatives of y in the case of Eq. (B4) are as follows:

$$\begin{aligned}
Ty_T &= \Big[2\Delta T^*(1+F)(1+B\Delta T^*)^{-1} - B\Delta T^{*2}(1+f)(1+B\Delta T^*)^{-2} \\
&\quad + C\Delta\rho^{*2}A(1+D\Delta\rho^*)^{-1}\Big]T/T_c \\
T^2y_{TT} &= \Big[2(1+F)(1+B\Delta T^*)^{-1} - 4B\Delta T^*(1+F)(1+B\Delta T^*)^{-2} \\
&\quad + 2B^2\Delta T^{*2}(1+F)(1+B\Delta T^*)^{-3}\Big]T^2/T_c^2 \\
\rho y_\rho &= \Big[\Delta T^{*2}F_1(1+B\Delta T^*)^{-1} + 2C\Delta\rho^*(1+E+A\Delta T^*)(1+D\Delta\rho^*)^{-1} \\
&\quad + C\Delta\rho^{*2}(E_1+A_1\Delta T^*)(1+D\Delta\rho^*)^{-1} \\
&\quad - DC\Delta\rho^{*2}(1+E+A\Delta T^*)(1+D\Delta\rho^*)^{-2}\Big]\rho/\rho_c \\
\rho^2y_{\rho\rho} &= \Big[\Delta T^{*2}F_2(1+B\Delta T^*)^{-1} + 2C(1+E+A\Delta T^*)(1+D\Delta\rho^*)^{-1} \\
&\quad + 4C\Delta\rho^*(E_1+A_1\Delta T^*)(1+D\Delta\rho^*)^{-1} \\
&\quad + C\Delta\rho^{*2}(E_2+A_2\Delta T^*)(1+D\Delta\rho^*)^{-1} \\
&\quad - 4DC\Delta\rho^*(1+E+A\Delta T^*)(1+D\Delta\rho^*)^{-2} \\
&\quad - 2DC\Delta\rho^{*2}(E_1+A_1\Delta T^*)(1+D\Delta\rho^*)^{-2} \\
&\quad + 2D^2C\Delta\rho^{*2}(1+E+A\Delta T^*)(1+D\Delta\rho^*)^{-3}\Big]\rho^2/\rho_c^2 \\
T\rho y_{T\rho} &= \Big[2\Delta T^*F_1(1+B\Delta T^*)^{-1} - B\Delta T^{*2}F_1(1+B\Delta T^*)^{-2} \\
&\quad + 2C\Delta\rho^*\cdot A(1+D\Delta\rho^*)^{-1} + C\Delta\rho^{*2}A_1(1+D\Delta\rho^*)^{-1} \\
&\quad - DC\Delta\rho^{*2}A(1+D\Delta\rho^*)^{-2}\Big]T\rho/(T_c\rho_c) \qquad \text{(B6)}
\end{aligned}$$

The new quantities here are $A_1 = \Sigma na_n\Delta\rho^{*n-1}$, $A_2 = \Sigma n(n-1)a_n\Delta\rho^{*n-2}$, $E_1 = \Sigma ne_n\Delta\rho^{*n-1}$, $E_2 = \Sigma n(n-1)e_n\Delta\rho^{*n-2}$, $F_1 = \Sigma nf_n\Delta\rho^{*n-1}$, and $F_2 = \Sigma n(n-1)f_n\Delta\rho^{*n-2}$.

APPENDIX C: THE SCALED FORMULATION

In using scaling on the restricted linear model, the free energy density as given in Eq. (24) involves the following quantities:

$$A_0^*(T^*) = -1 + A_1^*(\Delta T^*) + A_2^*(\Delta T^*)^2 + A_3^*(\Delta T^*)^3$$

$$\rho^* = V_c/V = \rho/\rho_c$$

$$\mu^*(\rho_c, T^*) = \mu_0^* + \mu_1^*(\Delta T^*) + \mu_2^*(\Delta T^*)^2 + \mu_3^*(\Delta T^*)^3$$

and

$$A_{\text{anom}}^* = r^{2-\alpha}ak\left[f_0 + f_2\theta^2 + f_4\theta^4\right] \tag{C1}$$

The coefficients involved are

$$\begin{aligned} f_0 &= -\left[\beta(\delta - 3) - b^2\alpha\gamma\right]/\left[2b^4(2-\alpha)(1-\alpha)\alpha\right] \\ f_2 &= \left[\beta(\delta - 3) - b^2\alpha(1 - 2\beta)\right]/\left[2b^2(1-\alpha)\alpha\right] \\ f_4 &= -(1-2\beta)/(2\alpha) \end{aligned} \tag{C2}$$

Here, α, β, γ, and δ are critical exponents, and a, k, and b^2 are termed linear model parameters. In the present calculations, the interrelations

$$\begin{aligned} \delta &= 1 + 2/\left(1 - b^2(1-2\beta)\right) \\ \gamma &= \beta(\delta - 1) \\ \alpha &= 2 - \beta(\delta + 1) \end{aligned} \tag{C3}$$

were used, with the numerical values $\beta = 0.3505$, $b^2 = 1.40991$, $a = 24.0999$, and $k = 1.6837$, which give $\delta = 4.457594$, $\gamma = 1.2118867$, and $\alpha = 0.087113297$. The special constants of "Set G" are $A_1^* = -7.874245$, $A_2^* = 25.844782$, $A_3^* = -3.96522$, $\mu_0^* = -11.295$, $\mu_1^* = -34.025$, $\mu_2^* = -14.35$, and $\mu_3^* = 10.4$. The similar constants of "Set K" are $A_1^* = -7.852192$, $A_2^* = 28.470406$, $A_3^* = -58.722451$, $\mu_0^* = -11.29$, $\mu_1^* = -34.05$, $\mu_2^* = -16.59$, and $\mu_3^* = 59.84$. The critical point constants of Levelt Sengers are 22.0477 MPa or 217.59388 atm, $\rho_c = 324.383\ \text{kg}\cdot\text{m}^{-3}$ or 403.68892 amagat, $V_c = 3.08279\ \text{cm}^3\cdot\text{g}^{-1}$, and $T_c = 647.073$ K (IPTS, 1969).

APPENDIX D: DETERMINATION OF r AND θ

A procedure was suggested by Moldover [11] for obtaining values for the parametric variables r and θ from the density ρ and temperature T. This involved an iterative solution of a transcendental equation

$$f(Z) = 0 = C + Z|1 - Z^2|^{-\beta} \tag{D1}$$

by Newton's method, with $C = -\Delta\rho^*(b/k)|\Delta T^*|^{-\beta}$, where $Z = b\theta$. A slowness of convergence near $Z = 1$ was adjusted for by special approximations, giving the initial value for Z suitably near 1 when ΔT^* is near zero.

Another form for the relationship of the previous transcendental equation is

$$f(Z) = 0 = D|Z|^{1/\beta} + Z^2 - 1 \tag{D2}$$

where $D = |C|^{-1/\beta}$. The iteration process by Newton's method then uses

$$Z_{n+1} = Z_n - \frac{[D|Z_n|^{1/\beta} + Z_n^2 - 1]}{[D|Z_n|^{1/\beta}/(\beta Z_n) + 2Z_n]} \tag{D3}$$

or

$$Z_{n+1} = Z_n - \beta Z_n \left\{ 1 - \frac{[(2\beta - 1)Z_n^2 + 1]}{[D|Z_n|^{1/\beta} + 2\beta Z_n^2]} \right\} \tag{D4}$$

With this form, there is no convergence problem near $Z = 1$. There is that problem, however, at a limiting value of Z, $Z_L = (1 - 2\beta)^{-1/2}$, at which the denominator for the Z increment goes to zero. The instability due to this can be removed by multiplying the increment indicated by a quantity going to zero at $Z = Z_L$ and staying close to unity elsewhere. $|1 - |Z/Z_L|^n|^m$ might do this for large n, and small m. A fairly satisfactory choice appears to be $n = 16$ and $m = 1/8$.

The same Z_L is a limiting value for the range of ρ and T that can be covered using the parametric variables. If $|Z|$ is increased beyond Z_L, the values of ρ and T that may be reached are values that could be reached with $|Z|$ less than Z_L. There is in this way a double-valued surface, but only the sheet with $|Z|$ less than Z_L is considered to have physical meaning. With the constants used for steam, the limiting value Z_L is 1.82879, which implies that θ must be within the range ± 1.54017.

The following FORTRAN subroutine, based on the preceding analysis, gives a way of calculating r and θ (as R and TH) in the case of simple scaling. Here T and RHO represents temperature and density, with TC and ROC as the critical point values. The quantities BTA, CK, and $B2$ are β, k, and b^2.

```
      SUBROUTINE RTHETA (T, RHO, R, TH, BTA, CK, B2, TC, ROC)
      IMPLICIT DOUBLE PRECISION (A - H, O - Z)
      ZL = 1./DSQRT(1.-2.*BTA)
      R = 0.D0
      TH = 0.D0
      TS = (T - TC)/TC
      RS = (RHO - ROC)/ROC
      B = DSQRT(B2)
      DS = (CK/B/DABS(RS))**(1./BTA)
      Z = (1.+(DABS(TS) - TS)/2./(1.+B)*DS*B**(1./BTA))*
    1 (1.+(DABS(TS) + TS)/2.*DS)**(-BTA)
      Z = Z*RS/(DABS(RS) + 1.D - 16)
      IF (Z) 100, 250, 100
  100 DO 200 N = 1, 20
      DBT = TS*DS*(DABS(Z))**(1./BTA)
      DZ = (DBT + Z**2 - 1.)/(DBT/Z/BTA + 2.*Z)
      DZ = DZ*DQSRT(DSQRT(DSQRT(DABS(1.-((Z/ZL)**4)**4))))
      Z = Z - DZ
      IF (Z**2 - ZL**2) 120, 250, 250
  120 IF (DABS(DZ/Z) - 1.D - 12) 250, 250, 150
  150 CONTINUE
  200 CONTINUE
  250 TH = Z/B
      R = TS/(1.-B2*TH**2)
      IF (R) 300, 350, 350
  300 WRITE (6, 1040) R
 1040 FORMAT (10X, 4HR   =   , E16.8)
  350 CONTINUE
      R = DABS(R)
      RETURN
      END
```

APPENDIX E: COMPUTATIONAL CONSIDERATIONS

The calculation of thermodynamic properties, including the effects of a switch function, may be in considerable measure a study in computer programming. A plausible procedure, starting with an indicated set of values of temperature and density, may proceed in the following way. If the temperature T is compared with the critical, T_c, and is found to be above it, then the "distance" s from the critical point is to be computed and compared with s_1 and s_2 to determine the value for the switch function g and its derivatives if needed. If s is less than s_2, then values for the parametric variables r and θ are required, based on the temperature T and density ρ. The calculation is then quite straightforward. On the other hand, if the temperature is below the critical temperature, there will be a first task of determining whether the system point is within or outside the vaporization dome. If it is not known to be outside, it may be necessary to compare the density with that of the saturated liquid or vapor. If it is between these two, then properties for both liquid and vapor are required.

In principle, for a limited range of temperature below T_c, the comparison might be made using scaling variables by at first taking $\theta = -1$ for the vapor and $\theta = +1$ for the liquid, with $r = \Delta T^*/(1 - b^2\theta^2)$ to estimate densities, but varying these for $s > s_1$, as needed to iterate to have equality for vapor and liquid in pressure and in Gibbs free energy. This further adjustment is required since use of the switching function, bringing in effects of the classical formulation, will move the saturation conditions away from $\theta = \pm 1$. The procedure with r and θ adjustment is usable for steam down to temperatures near 600 K, or nearly 50 deg below critical. At the limiting temperature, the actual saturation vapor density goes beyond even the limit for the metastable region for simple scaling, namely, $\theta \simeq 1.54$. Thus, the using of r and θ of simple scaling as an indicator of T and ρ becomes impossible at lower temperature. It may be noted that even negative vapor densities would be suggested by the simple scaling model for T less than 587.08 K. However, the regions in question are so far below the critical temperature that a purely classical formulation would be used anyway.

In one particular computation scheme compatible with using r and θ basically as adjustment variables, the certainty as to the temperature desired permits a primary use of r alone as an adjustment variable, with θ then given secondarily from the r and T values according to the relation for the linear scaling model

$$\theta = \pm\left[(1 - (T/TC - 1)/r)/b^2\right]^{1/2} \tag{E1}$$

with the sign determined by comparison between the density and its critical value. In case the desired values for density and temperature are known, it becomes expedient to have a procedure for determining the corresponding values of r and θ. This is carried out with a suitable subroutine for the computer program, as discussed in Appendix D.

A number of exploratory calculations were made in the single phase region along paths of constant specific volume using uniform steps in temperature. Each path was started at a chosen elevated temperature and then continued at successively lower temperatures until some chosen lower bound was reached, or until encountering the vaporization dome, where an attempt would occur at entry into the region of nonexistence of any scaled representation.

Another type of calculation to be considered is made with steps of rising temperature at constant density under conditions of equilibrium between vapor and liquid. This has application to a comparison with experimental data for the effective or apparent heat capacity at constant volume. Some details of the calculation in the coexistence region may be appropriate for special mention. A procedure for following a path of increasing temperature at constant density was prepared. The initial assigned values of temperature (no lower than ~600 K in the preliminary program) and (average) density are to be within the vaporization region. The substance then can be described as "wet steam." The program uses the accepted linear scaling relationship at first to make initial estimates of values for the parametric variables r and θ. Initial values $\theta_G = -1$ for the vapor and $\theta_L = +1$ for the liquid are assigned, and $r = \Delta T^*/(1 - b^2\theta^2)$ or $\Delta T^*/(1 - b^2)$ is calculated. This value of r is taken initially for both r_G for the vapor and r_L for the liquid. In general, these would be correct only according to the scaling model. An iteration loop for two independent and two dependent variables is then entered into in which the two parametric variables, r_G for the gas or vapor, and r_L for the liquid, are varied as independent variables, with the objective of bringing to zero the two differences

$$(-G/RT)_L - (-G/RT)_G \quad \text{and} \quad (P_L/P_C - P_G/P_C) \tag{E2}$$

These are to give equality of the Gibbs free energy G for liquid and vapor and also equality of pressure P for liquid and vapor. This is equivalent to the double tangent construction involving the Helmholtz free energy A plotted versus volume V. It can be regarded as formally equivalent to invoking the Maxwell condition, if that had been feasible. In the loop, a special subroutine is used twice, once with gas variables r_G, θ_G, etc., and once with liquid variables, r_L, θ_L, etc., on each passage. In accordance with the switch function chosen, it blends together function values for the scaled and the classical or analytic representations, with each given by a separate inner subroutine. The relation

$$\theta^2 = (1 - \Delta T^*/r)/b^2 \tag{E3}$$

is used, with r either as r_G or as r_L, while the θ resulting is taken with the appropriate sign according to whether it is for vapor or for liquid.

The classical inner subroutine responds directly to values of temperature T and density ρ. As set up, the scaled inner subroutine uses r and θ values to generate the anomalous contribution and also T and ρ values to give necessary reduced variables and to convert to units compatible with the classical functions. The blending subroutine makes use of another inner subroutine which contains details of the actual switch function employed. The list of arguments carried into this inner subroutine includes the assigned fixed values for s_1 and s_2, demarking the regions within which a calculated variable s for "distance" from the critical point will result in the switch function g having values $g = 1$, for $s < s_1$; $g = 0$, for $s > s_2$; or a value of g between 1 and 0, for $s_1 < s < s_2$.

This inner subroutine defines the dependence of s on the physical variables T and ρ, or equivalently on ΔT^* and $\Delta\rho^*$. It also supplies values for the necessary derivatives for contributions to thermodynamic functions. The iteration toward the condition of equality for the Gibbs free energy and for pressure for vapor and liquid phases is continued until satisfactory. The assigned density ρ is then compared with the densities of vapor and liquid at saturation. If it is between them, the fraction as vapor is taken as

$$x_G = \rho_G(\rho_L/\rho - 1)/(\rho_L - \rho_G) \tag{E4}$$

and the fraction as liquid as $x_L = 1 - x_G$. The internal energy, in units of the gas constant R, is then stored, in single array, based on

$$U/R = (x_G(E/RT)_G + x_L(E/RT)_L)T \tag{E5}$$

and the temperature T is similarly stored. However, if the density comparison shows that the assigned density is outside the vaporization dome, the action passes to the corresponding one of two differing parts of the program, involving an iteration loop with either a single calling of the subroutine for vapor or else one for liquid. For this, there is a single independent variable r_G, or else r_L, according to the region involved, and the dependent variable to be brought satisfactorily to zero is either $(\rho_V - \rho)/\rho_c$ or $(\rho_L - \rho)/\rho_c$ correspondingly. For successive points after the path of increasing temperature has emerged from the vaporization dome, the same part of the program with a single independent variable continues to be used. However, a single use of a subroutine to supply the needed r and θ is brought in before entering the iteration loop, by which the stated density as well as temperature can be complied with immediately. The quantities U/R and T continue to be stored in arrays as before. When the temperature range is completed, numerical differentiation gives the estimated C_v/R values.

REFERENCES

1. G. A. Chapela and J. S. Rowlinson, *Faraday Trans.* (*I*) **70**:584 (1974).
2. T. A. Murphy, J. V. Sengers, and J. M. H. Levelt Sengers, in *Proc. 8th Int. Conf. Properties of Water and Steam*, P. Bury, H. Perdon and B. Vodar, eds. (Editions Européennes Thermiques et Industries, Paris, 1975), p. 603.
3. J. M. H. Levelt Sengers, in *Proc. 7th Symp. Thermophys. Properties*, A. Cezairliyan, ed. (ASME, New York, 1977), p. 774.
4. J. Kestin, Informal remarks, Symposium on the Evaluation of Thermodynamic Properties of Fluids, Airlie House, Warrenton, Va., Nov. 4–7, 1969.
5. G. N. Lewis and M. Randall, *Thermodynamics*, 2nd ed. (McGraw-Hill, New York, 1961), pp. 301, 305; W. J. Moore, *Physical Chemistry*, 3rd ed. (Prentice-Hall, Englewood Cliffs, N.J., 1963), pp. 273, 274.
6. R. Pollak, in *Proc. 8th Int. Conf. Properties of Water and Steam*, P. Bury, H. Perdon, and B. Vodar, eds. (Editions Européennes Thermiques et Industries, Paris, 1974), p. 821.
7. R. Pollak, *The Thermodynamic Properties of Water up to* 1200 *K and* 3000 *Bar* (IUPAC Thermodynamic Tables Project Centre, London, 1976).
8. H. W. Woolley, in *Water and Steam*: *Their Properties and Current Industrial Applications*, J. Straub and K. Scheffler, eds. (Pergamon Press, Oxford, 1980), p. 166.
9. H. D. Baehr and H. Schomäcker, *Forsch. Ing. Wes.* **41**:43 (1975).
10. J. M. H. Levelt Sengers, B. Kamgar-Parsi, F. W. Balfour, and J. V. Sengers, *J. Phys. Chem. Ref. Data* **12**:1 (1983).
11. M. R. Moldover, *J. Res. NBS* **83**:329 (1978).